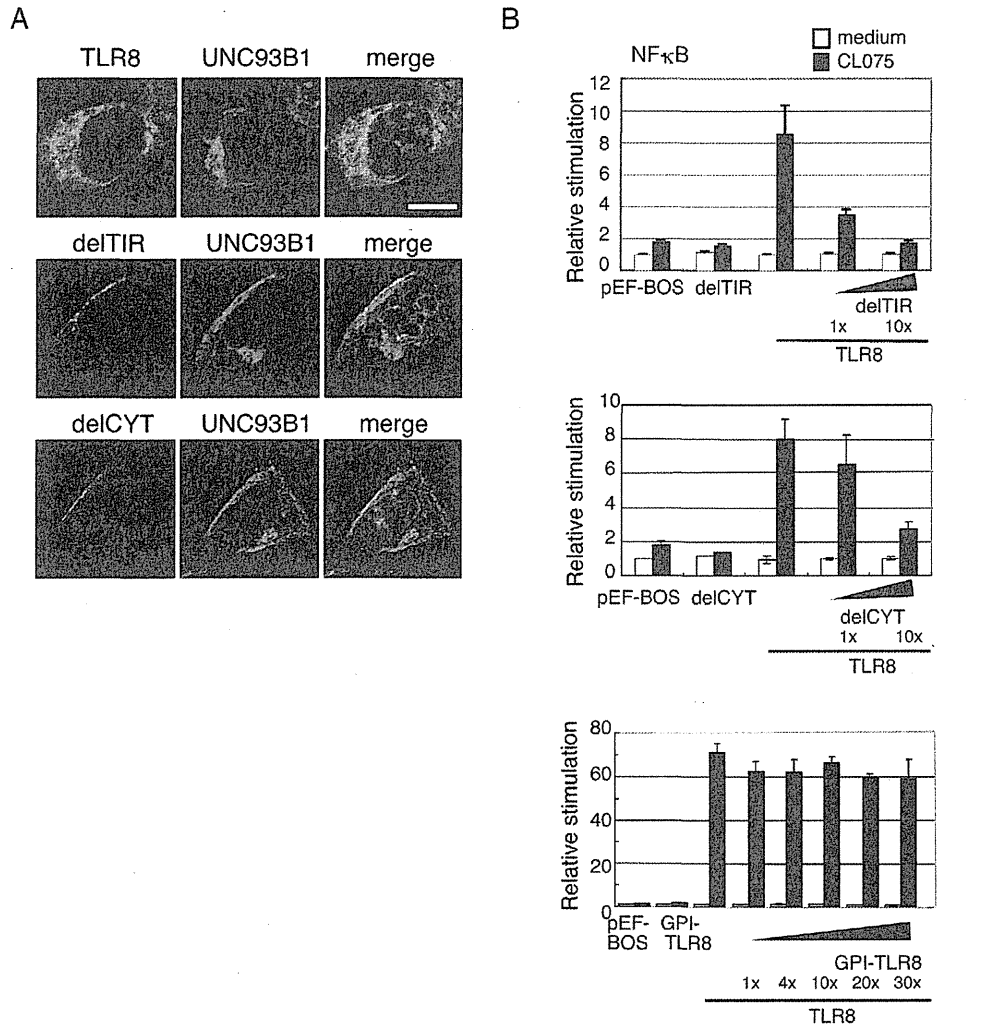

Figure 4. UNC93B1 colocalizes with surface-expressed TLR8 mutants. *A*, HeLa cells transiently expressing wild-type TLR8, delCYT, or delTIR were incubated with anti-FLAG mAb and anti-human UNC93B1 pAb followed by an Alexa Fluor 568-conjugated anti-mouse IgG and Alexa Fluor 488-conjugated anti-rabbit IgG. Representative confocal images are shown. Green, endogenous UNC93B1; red, TLR8; blue, nuclei stained with DAPI. Scale bar:10 μm. *B*, Surface-expressed TLR8 mutant proteins inhibited CL075-induced TLR8-mediated NF-κB activation. Luciferase activity of HEK293 cells transfected with the ELAM-promoter-luciferase reporter and expression plasmid for wild-type TLR8 together with increasing amounts of plasmid expressing delTIR (upper graph), delCYT (middle graph), or GPI-TLR8 (lower graph). Twenty-four hours after transfection, the cells were stimulated with 2.5 μg/mL of CL075 or left untreated. After 24 hours, the luciferase reporter activities were measured and expressed as the fold induction relative to the activity of unstimulated cells. Representative data from a minimum of three separate experiments are shown (mean and s.d. of triplicate assays).
doi:10.1371/journal.pone.0028500.g004

anti-LAMP-1 mAb (Biolegend), anti-MPR pAb (Abcam, Cambridge, UK), anti-human TLR8 mAb (Dendritics, LYON, France) and anti-human UNC93B1 pAb (ProSci Inc., Poway, CA). Lysotracker was from Invitrogen. CL075 was from InvivoGen.

Plasmids

Complementary DNAs for human TLR3 and TLR8 were cloned in our laboratory by RT-PCR from the mRNA of monocyte-derived immature DCs and were ligated into the cloning site of the expression vector, pEF-BOS, which was provided by Dr. S. Nagata (Kyoto University). The FLAG-tag or HA-tag was inserted into the C-terminal of pEF-BOS expression vectors for hTLR3 or hTLR8. The truncated TLR8 mutants, delTIR (1-896 a.a.) and delCYT (1-866 a.a.) were generated by PCR with Pfu Turbo DNA polymerase (STRATAGENE) using specific primers (forward primer; 5′-GACTACAAAGACGATGACGACAAGTAAGCG-3′, reverse primer for delTIR; 5′-GAAAGTTTGCGATGTGGAAAGAGACCTGTA-3′, reverse primer for delCYT; 5′-AGCCAGGGCAGCCAACATAACCATGGTGGT-3′) as described [21]. GPI-hTLR8 was constructed in the pEF-BOS expression vector by ligation of PCR products corresponding to the TLR8 ectodomain (45-843 a.a.) sequentially attached with the preprotrypsin signal sequence, HAT, and Flag at the N-terminus, and the GPI-attachment sequence from CD55 at

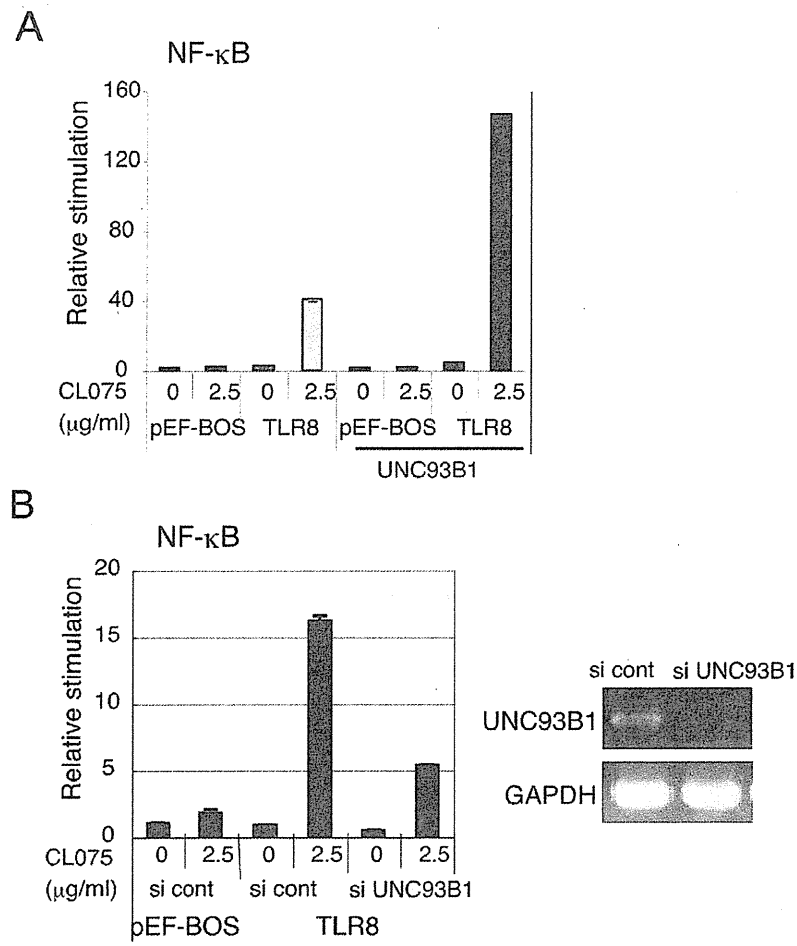

Figure 5. UNC93B1 is indispensable for TLR8-mediated signaling. *A*, Upregulation of TLR8-mediated NF-κB activation by co-expression with UNC93B. HEK293 cells were transfected with the indicated plasmid together with the ELAM reporter plasmid. Twenty-four hours after transfection, the cells were stimulated with CL075 or left untreated. After 6 hours, the luciferase reporter activities were measured and expressed as the fold induction relative to the activity of unstimulated cells. Representative data from three separate experiments are shown. *B*, TLR8-mediated NF-κB activation is downregulated by knockdown of UNC93B1. UNC93B1 siRNA or negative control siRNA was transfected into HEK293 cells together with the reporter plasmids and TLR8 expression plasmid. Forty-eight hours after transfection, cells were stimulated with CL075 for 6 hours and the luciferase reporter activities were measured. Data are representative of three independent experiments (mean and s.d. of triplicate assays). The expression of endogenous UNC93B1 and GAPDH mRNAs were examined using RT-PCR 48 hours after siRNA transfection (right panels).
doi:10.1371/journal.pone.0028500.g005

the C-terminus. The TLR4/TLR8 chimeric receptor, TLR4ecto/8, was constructed in the expression vector pEF-BOS by ligation of PCR products corresponding to amino acids 1-633 of human TLR4 ectodomain and amino acids 844-1059 of human TLR8. Another TLR4/TLR8 chimeric receptor, TLR4/8TIR, was constructed by the ligation of PCR products corresponding to amino acids 1-672 of human TLR4 (ectodomain, TM, and linker region) and amino acids 897-1059 of the human TLR8 TIR domain. Both constructs were FLAG tagged at the C-terminus. A plasmid for human UNC93B1 (pMD2/UNC93B1) and the expression plasmid for TLR4 (pEF-BOS/TLR4) were provided by Dr. K. Miyake (The University of Tokyo). The HA-tag was inserted into the C-terminal of the pEF-BOS expression vector for human UNC93B1. The human UNC93B1 mutant, hUNC93B1(H412R), in which the arginine residue at position 412 was substituted for a histidine residue, was made by site-directed mutagenesis.

Confocal microscopy

HeLa cells (1.0×10^5 cells/well) were plated onto micro cover glasses (Matsunami, Tokyo, Japan) in a 24-well plate. The following day, cells were transfected with the indicated plasmids using Fugene HD (Roche Diagnostics) or Lipofectamine 2000 (Invitrogen). Twenty-four hours after transfection, cells were fixed with 3% formalin for 30 min and permeabilized with PBS containing 0.5% saponin and 1% BSA for 30 min or fixed with 4% paraformaldehyde for 30 min and permeabilized with PBS containing 0.2% Triton X-100 and 1% BSA for 15 min (for staining of endogenous UNC93B1). In the case of monocytes, cells were fixed with 4% paraformaldehyde for 15 min. For the staining of late endosome, cells were permeabilized with PBS containing 100 μg/ml of digitonin and 1% BSA for 30 minutes. Fixed cells were blocked in PBS containing 1% BSA, and were then labeled with the indicated primary Abs (2~10 μg/ml) for 60 min at room temperature. Alexa-conjugated secondary Abs (1:400) were used

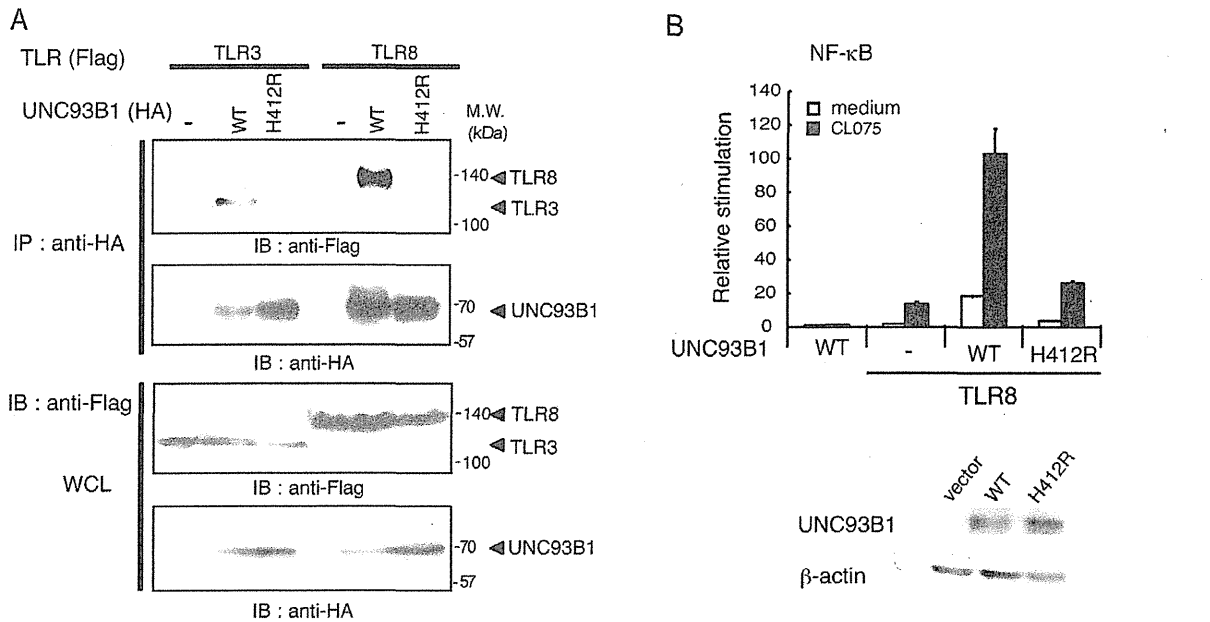

Figure 6. His412 is essential for the interaction of UNC93B1 with TLR8 and TLR8-mediated signaling. *A*, HEK293FT cells were transfected with the corresponding vectors for expression of the indicated proteins. The cell lysates were immunoprecipitated (IP) with anti-HA pAb, resolved by SDS-PAGE and detected by immunoblotting (IB) with anti-FLAG M2 or anti-HA mAb. Whole cell lysates (WCL) were subjected to immunoblotting with anti-FLAG or anti-HA mAb to detect protein expression. Molecular weight markers are shown on the right. *B*, HEK293 cells were transfected with the indicated plasmid together with the ELAM reporter plasmid. Cells were stimulated with CL075 or left untreated and the luciferase reporter activities were measured. Representative data from three separate experiments are shown. *Lower panels*, protein expression of wild-type and mutant UNC93B1 in HEK293 cells. β-actin blots are shown as loading controls.
doi:10.1371/journal.pone.0028500.g006

to visualize the staining of the primary Abs. After mounting with ProLong Gold with DAPI (Molecular Probes), cells were visualized at a magnification of ×63 with an LSM510 META microscope (Zeiss, Jena, Germany).

Reporter assay

HEK293 cells (5×10^5 cells/well) cultured in 24-well plates were transfected with the indicated plasmid together with the reporter plasmid and an internal control vector, phRL-TK (Promega), using FuGENE HD. The reporter plasmid containing the ELAM-1 promoter was constructed in our laboratory. Twenty-four hours after transfection, cells were stimulated with 2.5 μg/mL CL075. The cells were collected 6 hours after stimulation and then lysed. The *Firefly* and *Renilla* luciferase activities were determined using a dual-luciferase reporter assay kit (Promega). The *Firefly* luciferase activity was normalized with the *Renilla* luciferase activity and was expressed as the fold induction relative to the activity in unstimulated vector-transfected cells. All assays were performed in triplicate.

RNAi

siRNA duplexes (UNC93B1:ID #s37730, negative control: catalog #AM4635) were obtained from Ambion-Applied Biosystems. HEK293 cells cultured in 24-well plates were transfected with 20 pmol of each siRNA together with the expression vector for hTLR8 (40 ng), ELAM reporter plasmid (60 ng), an internal control vector (1.5 ng) and empty vector (400 ng) using Lipofectamin 2000. Forty-eight hours after transfection, cells were washed once and then stimulated with 2.5 μg/ml CL075 for 6 hours. Knockdown of UNC93B1 was confirmed 48 hours after siRNA transfection by RT-PCR using specific primers (UNC93B1: forward primer 5′-GCCCATGATTTATTTCCTGAACCACTACC-3′ and reverse primer, 5′-GTGTGCTGAGTCCAGTCTTGTTCAG-3′, GAPDH: forward primer 5′-GAGTCAACGGATTTGGTCGT-3′ and reverse primer 5′- TTGATTTTGGAGGGATCTCG-3′). Experiments were repeated three times for confirmation of the results.

Immunoprecipitation

HEK293FT cells (2.5×10^5 cells/well) cultured in 12-well plates were transfected with the indicated plasmids using Lipofectamine 2000 (Invitrogen). After 24 hours, cells were washed twice with DPBS. Washed cells were lysed in 1% digitonin lysis buffer (50 mM Tris-HCl (pH 7.4), 150 mM NaCl, 5 mM EDTA, 2 mM PMSF, and a protease inhibitor cocktail) or 1% NP-40 lysis-washing buffer (50 mM Tris-HCl (pH 7.4), 150 mM NaCl, 10 mM EDTA, 1 mM PMSF, and a protease inhibitor cocktail) in Fig. 2. Lysates were clarified by centrifugation, pre-cleared with Protein G-Sepharose (GE Healthcare, Buckinghamshire, UK), and incubated with anti-FLAG mAb or anti-HA pAb. The immunoprecipitates were recovered by incubation with Protein G-Sepharose, washed three times with 0.1% digitonin washing buffer (50 mM Tris-HCl (pH 7.4), 150 mM NaCl, 5 mM EDTA, 1 mM PMSF) or 1% NP-40 lysis-washing buffer and then resuspended in denaturing buffer. Samples were analyzed by SDS-PAGE under reducing conditions followed by immunoblotting with anti-tag Abs.

Supporting Information

Figure S1 Flow cytometric analysis of cell surface expression of GPI-hTLR8 transiently expressed in HeLa cells. HeLa cells were

transfected with the empty vector or the expression plasmid for FLAG-tagged GPI-hTLR8 using Lipofectamine 2000 in 12-well plates. Twenty-four hours after transfection, cells were washed and incubated with anti-FLAG M2 mAb or mouse IgG1 in the presence of human IgG for 30 min at 4° C in FACS buffer (DPBS containing 0.5% BSA and 0.1% sodium azide). Cells were washed twice in FACS buffer and incubated with FITC-labeled secondary antibody (American Qualex) for 30 min at 4° C. For intracellular staining, cells were permeabilized with permeabilizing solution (BD) for 10 min at room temperature, and then stained with anti-FLAG mAb in the presence of 10% goat serum and FITC-labeled secondary Ab. Cells were analyzed using a FACS Calibur (BD). Shaded histogram: control mouse IgG 1 staining; thick line: anti-FLAG mAb staining. Inset values indicate the mean fluorescent intensities specific for the anti-FLAG mAb.
(EPS)

Figure S2 Forced expression of TLR8 mutants affects the endosomal localization of wild-type TLR8. *A*, Confocal images show HeLa cells co-expressing HA-tagged wild-type TLR8 and FLAG-tagged TLR8 mutants. Cells were fixed and stained with anti-FLAG mAb and anti-HA pAb, followed by Alexa568-labeled goat anti-mouse Ab and Alexa488-labeled goat anti-rabbit Ab. TLR8 mutants delCYT and delTIR were anchored on plasma membrane and did not merge with wild-type TLR8. Red, TLR8 mutants; green, wild-type TLR8; blue, nuclei stained with DAPI; bar, 10 μm. *B*, Cells were transfected with FLAG-tagged wild-type TLR8 alone (upper panels), together with FLAG-tagged delCYT (middle panels) or FLAG-tagged delTIR (lower panels), and stained with anti-FLAG mAb and anti-EEA1 pAb, followed by Alexa568-labeled goat anti-mouse Ab and Alexa488-labeled goat anti-rabbit Ab. Wild-type TLR8 was expressed intracellularly and colocalized with EEA1 (upper panels). When delCYT or delTIR was expressed with wild-type TLR8, colocalization between TLR8 and EEA1 was decreased (middle and lower panels). Red, TLR8; green, early endosome marker EEA1; blue, nuclei stained with DAPI; bar, 10 μm.
(EPS)

Acknowledgments

We are grateful to Drs. H. Oshiumi, H. Shime, T. Ebihara, A. Matsuo, H. H. Aly, H. Takaki, and J. Kasamatsu for invaluable discussions. Thanks are also due to Dr. K. Miyake (University of Tokyo, Tokyo) for providing plasmids.

Author Contributions

Conceived and designed the experiments: HI KF TS MM. Performed the experiments: HI MT AW KI. Analyzed the data: MT TS MM. Wrote the paper: MM.

References

1. Medzhitov R, Janeway CA, Jr. (1997) Innate immunity: the virtues of a nonclonal system of recognition. Cell 91: 295–298.
2. Akira S, Uematsu S, Takeuchi O (2006) Pathogen recognition and innate immunity. Cell 124: 783–801.
3. Kono H, Rock KL (2008) How dying cells alert the immune system to danger. Nat Rev Immunol 8: 279–289.
4. Medzhitov R, Preston-Hurlburt P, Janeway CA, Jr. (1997) A human homologue of the Drosophila Toll protein signals activation of adaptive immunity. Nature 388: 394–397.
5. Muzio M, Bosisio D, Polentarutti N, D'amico G, Stoppacciaro A, et al. (2000) Differential expression and regulation of toll-like receptors (TLR) in human leukocytes: selective expression of TLR3 in dendritic cells. J Immunol 164: 5998–6004.
6. Kadowaki M, Ho S, Antonenko S, de Waal Malefyt R, Kastelein RA, et al. (2001) Subsets of human dendritic cell precursors express different Toll-like receptors and respond to different microbial antigens. J Exp Med 194: 863–870.
7. Hornung V, Rothenfusser S, Britsch S, Krug A, Jahrsdorfer B, et al. (2002) Quantitative expression of Toll-like receptor 1-10 mRNA in cellular subsets of human peripheral blood mononuclear cells and sensitivity to CpG oligodeoxynucleotides. J Immunol 168: 4531–4537.
8. Matsumoto M, Funami K, Tanabe M, Oshiumi H, Shingai M, et al. (2003) Subcellular localization of Toll-like receptor 3 in human dendritic cells. J Immunol 171: 3154–3162.
9. Chuang T-H, Ulevitch RJ (2000) Cloning and characterization of a sub-family of human Toll-like receptors: hTLR7, hTLR8 and hTLR9. Eur Cytokine Netw 11: 372–378.
10. Du X, Poltorak A, Wei Y, Beutler B (2000) Three novel mammalian toll-like receptors: gene structure, expression, and evolution. Eur Cytokine Netw 11: 362–371.
11. Heil F, Hemmi H, Hochrein H, Ampenberger F, Kirschning C, et al. (2004) Species-specific recognition of single-stranded RNA via toll-like receptor 7 and 8. Science 303: 1526–1529.
12. Diebold SS, Kaisho T, Hemmi H, Akira S, Sousa RC (2004) Innate antivial responses by means of TLR7-mediated recognition of single-stranded RNA. Science 303: 1529–1531.
13. Gorden KB, Gorski KS, Gibson SJ, Kedl RM, Kieper WC, et al. (2005) Synthetic TLR agonists reveal functional differences between human TLR7 and TLR8. J Immunol 174: 1259–1268.
14. Jurk M, Heil F, Vollmer J, Schetter C, Krieg AM, et al. (2002) Human TLR7 or TLR8 independently confer responsiveness to the antiviral compound R-848. Nat Immunol 3: 499.
15. Ma Y, Li J, Chiu I, Wang Y, Sloane JA, et al. (2006) Toll-like receptor 8 functions as a negative regulator of neurite outgrowth and inducer of neuronal apoptosis. J Cell Biol 28: 209–215.
16. Peng G, Guo Z, Kiniwa Y, Voo KS, Peng W Fu, et al. (2005) Toll-like receptor 8-mediated reversal of CD4+ regulatory T cell function. Science 309: 1380–1384.
17. Jongbloed SL, Kassianos AJ, McDonald KJ, Clark GJ, Ju X, et al. (2010) Human CD141+ (BDCA-3+) dendritic cells (DCs) represent a unique myeloid DC subset that cross-presents necrotic cell antigens. J Exp Med 207: 1247–1260.
18. Oshiumi H, Matsumoto M, Funami K, Akazawa T, Seya T (2003) TICAM-1, an adaptor molecule that participates in Toll-like receptor 3-mediated interferon-beta induction. Nat Immunol 4: 161–167.
19. Yamamoto M, Sato S, Hemmi H, Hoshino K, Kaisho T, et al. (2003) Role of adaptor TRIF in the MyD88-independent Toll-like receptor signaling pathway. Science 301: 640–643.
20. Funami K, Sasai M, Ohba Y, Oshiumi H, Seya T, et al. (2007) Spatiotemporal mobilization of Toll/IL-1 receptor domain-containing adaptor molecule-1 in response to dsRNA. J Immunol 179: 6867–6872.
21. Funami K, Matsumoto M, Oshiumi H, Akazawa T, Yamamoto A, et al. (2004) The cytoplasmic 'linker region' in Toll-like receptor 3 controls localization and signaling. Int Immunol 16: 1143–1154.
22. Nishiya T, DeFranco AL (2004) Ligand-regulated chimeric receptor approach reveals distinctive subcellular localization and signaling properties of the Toll-like receptors. J Biol Chem 279: 19008–19017.
23. Barton GM, Kagan JC, Medzhitov R (2006) Intracellular localization of Toll-like receptor 9 prevents recognition of self DNA but facilitates access to viral DNA. Nat Immunol 7: 49–56.
24. Brinkmann MM, Spooner E, Hoebe K, Beutler B, Ploegh HL, et al. (2007) The interaction between the ER membrane protein UNC93B and TLR3, 7, and 9 is crucial for TLR signaling. J Cell Biol 177: 265–275.
25. Kim Y-M, Brinkmann MM, Paquet M-E, Ploegh HL (2008) UNC93B1 delivers nucleotide-sensing toll-like receptors to endolysosomes. Nature 452: 234–238.
26. Ewald SE, Lee BL, Lau L, Wickliffe KE, Shi G-P, et al. (2008) The ectodomain of Toll-like receptor 9 is cleaved to generate a functional receptor. Nature 456: 658–662.
27. Park B, Brinkmann MM, Spooner E, Lee CC, Kim YM, et al. (2008) Proteolytic cleavage in an endolysosomal compartment is required for activation of Toll-like receptor 9. Nat Immunol 9: 1407–141.
28. Fukui R, Saitoh S, Matsumoto F, Kozuka-Hara H, Oyama M, et al. (2009) Unc93B1 biases Toll-like receptor responses to nucleic acid in dendritic cells toward DNA- but against RNA-sensing. J Exp Med 206: 1339–1350.
29. Tabeta K, Hoebe K, Janssen EM, Du X, Georgel P, et al. (2006) The Unc93B1 mutation 3d disrupts exogeneous antigen presentation and signaling via Toll-like receptors 3, 7 and 9. Nat Immunol 7: 146–164.
30. Gibbard RJ, Morley, PJ, Gay NJ (2006) Conserved features in the extracellular domain of human Toll-like receptor 8 are essential for pH-dependent signaling. J Biol Chem 281: 27503–27511.
31. Leifer CA, Brooks JC, Hoelzer K, Lopez J, Kennedy MN, et al. (2006) Cytoplasmic Targeting motifs control localization of Toll-like receptor 9. J Biol Chem 281: 35585–35592.
32. Zhua J, van Drunen Littel-van den Hurka S, Brownliea R, Babiuka LA, Pottera A, et al. (2009) Multiple molecular regions confer intracellular localization of bovine Toll-like receptor 8. Molec Immunol 46: 884–892.

33. Matsumoto M, Seya T (2008) TLR3: Interferon induction by double-stranded RNA including poly(I:C). Adv Drug Del Rev 60: 805–812.

34. Ebihara T, Azuma M, Oshiumi H, Kasamatsu J, Iwabuchi K, et al. (2010) Identification of a polyI:C-inducible membrane protein that participates in dendritic cell-mediated natural killer cell activation. J Exp Med 207: 2675–2687.

Published October 12, 2011, doi:10.4049/jimmunol.1101503

The TLR3/TICAM-1 Pathway Is Mandatory for Innate Immune Responses to Poliovirus Infection

Hiroyuki Oshiumi,*,[1] Masaaki Okamoto,*,[1] Ken Fujii,[†] Takashi Kawanishi,* Misako Matsumoto,* Satoshi Koike,[†] and Tsukasa Seya*

Cytoplasmic and endosomal RNA sensors recognize RNA virus infection and signals to protect host cells by inducing type I IFN. The cytoplasmic RNA sensors, retinoic acid inducible gene I/melanoma differentiation-associated gene 5, actually play pivotal roles in sensing virus replication. IFN-β promoter stimulator-1 (IPS-1) is their common adaptor for IFN-inducing signaling. Toll/IL-1R homology domain-containing adaptor molecule 1 (TICAM-1), also known as TRIF, is the adaptor for TLR3 that recognizes viral dsRNA in the early endosome in dendritic cells and macrophages. Poliovirus (PV) belongs to the Picornaviridae, and melanoma differentiation-associated gene 5 reportedly detects replication of picornaviruses, leading to the induction of type I IFN. In this study, we present evidence that the TLR3/TICAM-1 pathway governs IFN induction and host protection against PV infection. Using human PVR transgenic (PVRtg) mice, as well as IPS-1$^{-/-}$ and TICAM-1$^{-/-}$ mice, we found that TICAM-1 is essential for antiviral responses that suppress PV infection. TICAM-1$^{-/-}$ mice in the PVRtg background became markedly susceptible to PV, and their survival rates were decreased compared with wild-type or IPS-1$^{-/-}$ mice. Similarly, serum and organ IFN levels were markedly reduced in TICAM-1$^{-/-}$/PVRtg mice, particularly in the spleen and spinal cord. The sources of type I IFN were CD8α^{+}/CD11c^{+} splenic dendritic cells and macrophages, where the TICAM-1 pathway was more crucial for PV-derived IFN induction than was the IPS-1 pathway in ex vivo and in vitro analyses. These data indicate that the TLR3/TICAM-1 pathway functions are dominant in host protection and innate immune responses against PV infection. *The Journal of Immunology*, **2011, 187: 000–000.**

When RNA viruses infect mammalian cells, type I IFN is generated to suppress viral infection. IFN-inducing pathways evoked by viral dsRNA have been identified in humans and mice, and the possible involvement of these pathways in protection against viruses has been examined using gene-disrupted mice and various virus species (1). The sensing of dsRNA by the innate immune system is accomplished either by TLR3 or by cytoplasmic sensors such as dsRNA-dependent protein kinase (so-called PKR), retinoic acid inducible gene I (RIG-I), and melanoma differentiation-associated gene 5 (MDA5) (2). In virus-infected cells, RIG-I and MDA5 mainly participate in type I IFN induction in conjunction with the adaptor molecule IFN-β promoter stimulator-1 (IPS-1; also known as MAVS, Cardif, or VISA) (1). The role of these molecules in host cell protection has been clearly delineated in RNA virus infection.

Toll/IL-1R homology domain-containing adaptor molecule 1 (TICAM-1; also called TRIF) is the adaptor of TLR3 (3–5). When TLR3 senses dsRNA on the endosomal membrane, it induces type I IFN (6, 7). The adaptor TICAM-1 plays a pivotal role in TLR3-mediated IFN-α/β induction. Once dsRNA stimulates TLR3, TICAM-1 transiently couples with TLR3 and forms a multimer, translocating to a distinct region of the cytoplasm (8). In its multimeric form, TICAM-1 recruits the kinase complex to activate IFN regulatory factors (IRF)-3 and -7, which induce type I IFN production (7, 9). Historically, this IFN-inducing pathway was identified earlier than the cytoplasmic RIG-I/MDA5 pathway (10, 11). Many reports have mentioned the possibility that the TLR3/TICAM-1 pathway is involved in the anti-viral IFN response (12), but no definitive evidence of the anti-viral properties of this pathway has been obtained using TICAM-1$^{-/-}$ mice (13). Only a DNA virus, mouse CMV (MCMV), has been shown to infect TICAM-1$^{-/-}$ mice, and thus mouse cells are partly protected from MCMV by the TICAM-1 pathway (5, 14).

Poliovirus (PV) is a positive strand ssRNA virus that produces dsRNA intermediates during viral replication (15), modified with 5′ terminal Vpg protein (16), a characteristic feature of picornaviruses. It is generally accepted that picornaviruses are recognized by MDA5 but not RIG-I in infected cells, presumably due to the generation of this unusual dsRNA. This concept was confirmed by the finding that MDA5$^{-/-}$ mice fail to induce type I IFN in response to encephalomyocarditis virus (EMCV) and permit severe EMCV infection (13, 17). However, another picornavirus, coxsackie B virus (CBV) serotype 3, is recognized by TLR3 in infected cells and induces IFN-γ as an effector for suppressing CBV infection

*Department of Microbiology and Immunology, Hokkaido University Graduate School of Medicine, Sapporo 060-8638, Japan; and [†]Department of Microbiology and Immunology, Tokyo Metropolitan Institute for Neuroscience, Tokyo Metropolitan Organization for Medical Research, Tokyo 156-0057, Japan

[1]H.O. and M.O. contributed equally to this work.

Received for publication May 24, 2011. Accepted for publication September 6, 2011.

This work was supported in part by Grants-in-Aid from the Ministry of Education, Science, and Culture of Japan (Specified Project for Advanced Research), the Ministry of Health, Labor, and Welfare of Japan, the Takeda Foundation, and by the Waxmann Foundation. Financial support by the Program of Founding Research Centers for Emerging and Reemerging Infectious Diseases, Ministry of Education, Culture, Sports, Science, and Technology of Japan, is gratefully acknowledged.

Address correspondence and reprint requests to Prof. Tsukasa Seya, Department of Microbiology and Immunology, Graduate School of Medicine, Hokkaido University, Kita-ku, Kita-15 Nishi-17, Sapporo, Hokkaido 060-8638, Japan. E-mail address: seya-tu@pop.med.hokudai.ac.jp

The online version of this article contains supplemental material.

Abbreviations used in this article: BM, bone marrow; BM-DC, bone marrow-derived dendritic cell; BM-Mf, bone marrow-derived macrophage; CBV, coxsackie B virus; DC, dendritic cell; EMCV, encephalomyocarditis virus; HCV, hepatitis C virus; IFIT-1, IFN-induced protein with tetratripeptide repeats 1; IP-10, IFN-γ–induced protein 10; IPS-1, IFN-β promoter stimulator-1; IRF, IFN regulatory factor; KO, knockout; MCMV, mouse cytomegalovirus; MDA5, melanoma differentiation-associated gene 5; MEF, mouse embryonic fibroblast; Mf, macrophage; MOI, multiplicity of infection; PV, poliovirus; PVRtg, poliovirus receptor transgenic; RIG-I, retinoic acid inducible gene I; RT-qPCR, real-time quantitative PCR; TICAM-1, Toll/IL-1R homology domain-containing adaptor molecule 1; WNV, West Nile virus; WT, wild-type.

www.jimmunol.org/cgi/doi/10.4049/jimmunol.1101503

(18). In this study, we analyzed in vivo infection of a popular picornavirus, PV, using PVR transgenic (PVRtg) mice, which show a neurotropic phenotype during PV infection similar to humans (19, 20). Using this mouse model, in combination with TICAM-1$^{-/-}$ or IPS-1$^{-/-}$ mice, we present evidence that the host TICAM-1 pathway, particularly in macrophages (Mf), serves as a source of type I IFN induction and protects host PVRtg mice from PV infection and paralytic death. Thus, the strategy for host protection against picornaviruses is not simply based on the MDA5-dependent dsRNA recognition, but is variable depending on picornavirus species.

Materials and Methods

Mice

All mice were backcrossed with C57BL/6 mice more than seven times before use. TICAM-1$^{-/-}$ (21) and IPS-1$^{-/-}$ mice (this study) were generated in our laboratory. TLR3$^{-/-}$ (4), IRF-3$^{-/-}$, and IRF-7$^{-/-}$ mice (22) were provided by Drs. S. Akira (Osaka University, Osaka, Japan) and T. Taniguchi (University of Tokyo, Tokyo, Japan). PVRtg mice were provided as reported previously (20). All mice were maintained under specific pathogen-free conditions in the Animal Facility at Hokkaido University Graduate School of Medicine (Sapporo, Japan). Animal experiments were performed according to the guidelines set by the Animal Safety Center, Japan.

Generation of IPS-1–deficient mice

The *IPS-1* gene was amplified by PCR using genomic DNA extracted from embryonic stem cells. The targeting vector was constructed by replacing the second and third exons with a neomycin-resistance gene cassette (Neo), and an HSV thymidine kinase driven by the PGK promoter was inserted into the genomic fragment for negative selection. After the targeting vector was transfected into 129/Sv mice-derived embryonic stem cells, G418 and ganciclovir doubly resistant colonies were selected and screened by PCR. The targeted cell line was injected into C57BL/6 blastocysts, resulting in the birth of male chimeric mice. These mice were then backcrossed with C57BL/6 mice. The disruption of the *IPS-1* gene was confirmed by PCR for the long and short arms. The abolishment of IPS-1 mRNA expression was confirmed by real-time quantitative PCR (RT-qPCR).

Cells, viruses, and reagents

Wild-type (WT) and TICAM-1$^{-/-}$ mouse embryonic fibroblasts (MEF) were prepared from 12.5- to 13.5-d-old embryos. PV, strain Mahoney, was amplified in Vero cells, and the viral titer was determined by a plaque assay. Bone marrow (BM) cells were prepared from the femur and tibia. The cells were cultured in RPMI 1640 (Invitrogen, New York, NY) supplemented with 10% FCS, 100 μM 2-ME, and 10 ng/ml murine GM-CSF or the culture supernatant of NIH3T3 cells expressing M-CSF. After 6 d, cells were collected and used as bone marrow-derived dendritic cells (BM-DC) or BM-derived macrophages (BM-Mf). For the preparation of BM-DC and BM-Mf, the medium was changed every 2 d. Splenic DC and NK cells were isolated using the MACS system (Miltenyi Biotec, Auburn, CA).

Experimental infection of mice

Five- to 8-wk-old C57BL/6 female mice were used throughout this study. Mice of different genotypes were i.p. or i.v. infected with PV at the doses indicated. The viability of the infected mice was monitored for 2 wk. We collected sera from the mice at different time points to measure viral titers by a plaque assay and cytokine levels by an ELISA. To determine the tissue viral titer, mice were euthanized and organs were aseptically removed and frozen by liquid nitrogen. Because the organs were not perfused before organs were removed, virus titers were determined including blood. Specimens were homogenized in 2 ml PBS on ice, and titers were determined by a plaque assay.

ELISA

Culture supernatants of cells (10^5) seeded on 24-well plates or sera were collected and analyzed for cytokine levels with ELISA. ELISA kits for IFN-α and IFN-β were purchased from PBL Biomedical Laboratories. ELISA was performed according to the manufacturer's instructions.

qPCR

For qPCR, total RNA was extracted with TRIzol (Invitrogen), and 0.2–0.5 μg RNA was reverse-transcribed using a high-capacity cDNA transcription kit (Applied Biosystems, Piscataway, NJ) with random primers according to the manufacturer's instructions. qPCR was performed using a Step One real-time PCR system (Applied Biosystems).

In vivo blocking of NK activity

Mice (PVRtg and PVRtg/TICAM-1$^{-/-}$) were i.p. injected with 250 μg anti-NK1.1 Ab, asialoGM1 Ab, or control PBS as described previously (21). One day later, the mice were i.p. inoculated with 10^4 PFU PV. One to 7 d after PV injection, depletion of peripheral NK1.1$^+$ cells was confirmed by flow cytometry. Then, the mortality of the mice was monitored. In some experiments, the spleen cells were harvested and NK cells (DX5$^+$ cells) were positively isolated using the MACS system (Miltenyi Biotec). The DX5$^+$ NK cells were suspended in RPMI 1640 containing 10% FCS and mixed with ^{51}Cr-labeled B16D8 cells at the indicated E:T ratios. After 4 h, the supernatants were harvested and [^{51}Cr] release was measured.

Statistical analysis

Statistical significance of differences between groups was determined by the Student *t* test, and survival curves were analyzed by the log-rank test using Prism 4 for Macintosh software (GraphPad Software). Student *t* tests and χ^2 goodness-of-fit tests were performed using Microsoft Excel software and a χ^2 distribution table.

Results

TICAM-1 is essential for protection of PVRtg mice against PV infection

Mice lacking the *mda-5* gene abrogate the production of type I IFN in response to EMCV infection and are more susceptible to infection with EMCV (13, 17). Because EMCV is a picornavirus, it has been proposed that MDA5 is critical for sensing picornavirus infection. In infected cells, picornaviruses efficiently generate long dsRNA, which is recognized by the cytoplasmic dsRNA sensor MDA5 (23). The 5′ end of the PV genomic RNA is linked to a VPg protein (16), not to a 5′-triphosphate, a major ligand for another cytoplasmic RNA sensor, RIG-I (24, 25). Thus, we first tested, using the PVRtg mouse model (20), whether the mortality of PV-infected mice is affected by disruption of IPS-1 (Fig. 1*A*). Approximately 70% of WT (PVRtg) mice and ~40% of IPS-1$^{-/-}$ mice survived >10 d postinoculation at an i.p. dose of 2×10^4 PFU. No statistical significance between these two groups was detected (Fig. 1*A*). In the same experiments, TICAM-1$^{-/-}$ mice died within 5 d by paralysis (Fig. 1*B*).

We next investigated the effect of the route of PV infection on mortality in this mouse model. PV (2×10^3 PFU) was injected i.p. or i.v. into WT and TICAM-1 mice and their mortality was examined (Fig. 1*C*, 1*D*). All TICAM-1$^{-/-}$ mice died by paralysis within 7.5 d irrespective of the injection route. The significance of this early mortality rate of PV-infected TICAM-1$^{-/-}$ mice was supported by statistical analysis. The mortality rates were slightly high in WT mice compared with IPS-1$^{-/-}$ mice when PV loads in mice were not very high (Supplemental Fig. 1*A*). This tendency seemingly diminished by early death of IPS-1$^{-/-}$ mice with high doses of PV input. These data suggested that TICAM-1, rather than IPS-1 (or the sensors RIG-I and MDA5), is a critical factor in protecting mice from PV-mediated paralytic death. This conclusion was confirmed using RIG-I$^{-/-}$ and MDA5$^{-/-}$ mice with a PVRtg background (S. Abe, K. Fujii, and S. Koike, submitted for publication).

These results showed a discrepancy with previous indications that MDA5 is critical in picornavirus protection (13). We therefore tested the dose dependence of PV in the survival of WT versus TICAM-1$^{-/-}$ mice. Surprisingly, high doses of PV (2×10^5 and 2×10^6 PFU) induced paralytic death in all WT as well as TICAM-1$^{-/-}$ mice within 6 d (Fig. 2*A*, 2*B*). Thus, high doses of PV (>2×10^5 PFU) appear to overpower the TICAM-1 PV-protective activity in vivo, which confirmed previous findings using other picornaviruses (13). TICAM-1 was most effective in

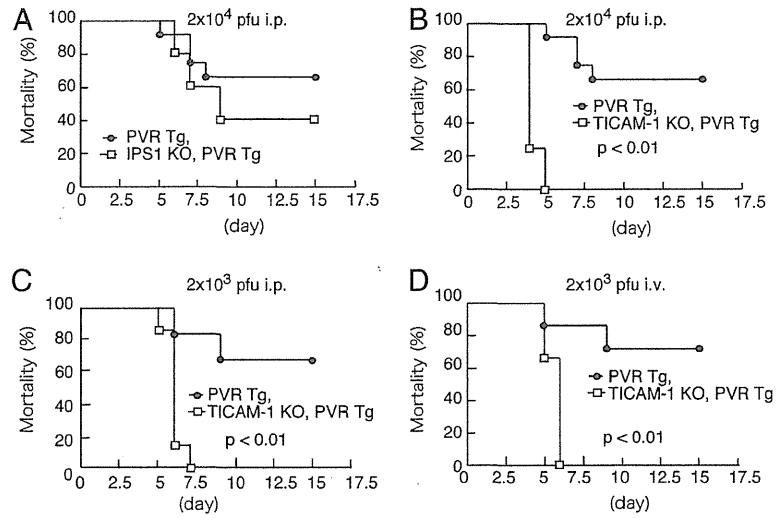

FIGURE 1. Survival of WT, TICAM-1 KO, and IPS-1 KO mice following i.p. or i.v. PV infection. *A* and *B*, PV (2×10^4 PFU) was infected via the i.p. route into WT and IPS-1 (*A*) or TICAM-1 (*B*) KO mice ($n \geq 5$), and survival was monitored for 14 d. *C* and *D*, PV (2×10^3 PFU) was infected via the i.p. (*C*) or i.v. (*D*) route into WT and TICAM-1 KO mice ($n \geq 5$), and survival was monitored for 14 d.

the survival against PV infection at low dose ($<2 \times 10^4$ PFU) (Figs. 1*B*, 1*C*, 2*C*). Similar results were obtained with the PV infection study (S. Abe, K. Fujii, and S. Koike, submitted for publication) when TICAM-$1^{-/-}$ mice were substituted with TLR3$^{-/-}$ or IRF-3/7 double-knockout (KO) mice. Results were confirmed using IRF-3$^{-/-}$ and IRF-7$^{-/-}$ mice (26). These results are essentially consistent with previous reports using a PVRtg/IFNAR$^{-/-}$ mouse model (27), in which type I IFN is critical for PV permissiveness, particularly in the intestine of PVRtg mice.

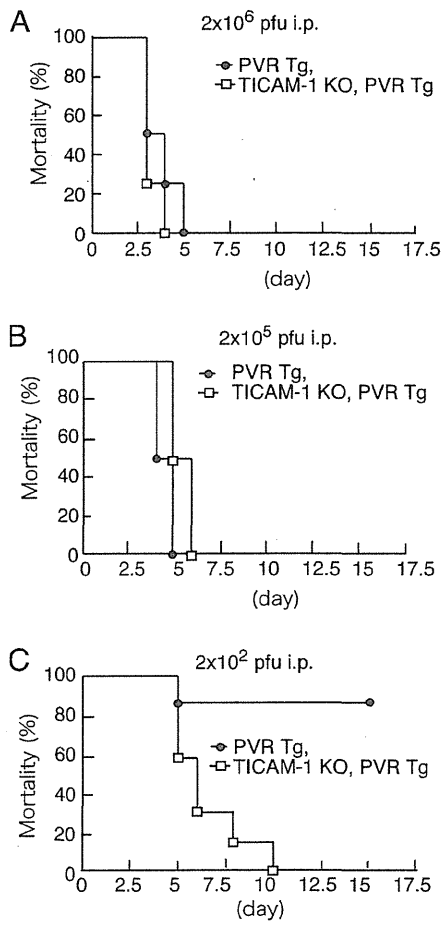

FIGURE 2. High doses of PV disable the protective effect of TICAM-1. WT and TICAM-1 KO mice ($n \geq 6$) were i.p. infected with 2×10^6 (*A*), 2×10^5 (*B*), or 2×10^2 PFU (*C*) PV and survival was monitored for 14 d.

TICAM-1–dependent type I IFN induction in PVRtg mice

PV titers in various organs were measured with WT and TICAM-$1^{-/-}$ mice i.p. injected with 2×10^4 PFU PV. In most organs, PV titers were higher in TICAM-$1^{-/-}$ mice than in WT mice at day 3 post-infection (Fig. 3*A*). The PV titer ratio in TICAM-$1^{-/-}$ versus WT mice was also high in the lung (Fig. 3*A*). In most organs except for the large intestine, high PV titers were harvested in TICAM-$1^{-/-}$ mice compared with WT mice. The difference in local PV titers between WT and TICAM-$1^{-/-}$ mice was culminated in the lung and spinal cord (Fig. 3*A*). Serum PV titers were increased within 48 h

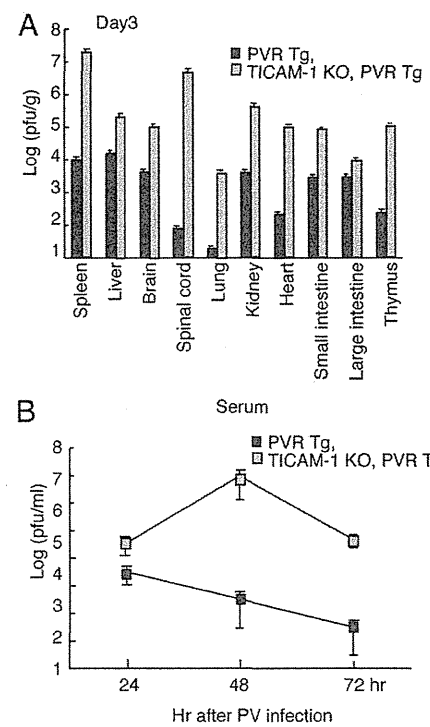

FIGURE 3. Viral titers in organs and serum following PV infection. WT and TICAM-1 KO mice were infected i.p. with 2×10^4 PFU PV. The viral titers in each organ (*A*) and sera (*B*) were measured by a plaque assay. Data are shown as means ± SD of three independent samples.

after PV i.p. injection in TICAM-$1^{-/-}$ mice compared with WT mice (Fig. 3*B*).

IFN-α/β levels were measured with sera from WT, IPS-$1^{-/-}$, and TICAM-$1^{-/-}$ mice, but they were barely detected in these PV-infected mice (Supplemental Fig. 1*B*). Only i.v. injection of high PV titers (an example shows $>4 \times 10^6$ PFU) allowed WT mice to release type I IFN within 12 h (Supplemental Fig. 1*B*). No IFN was detected in blood in TICAM-$1^{-/-}$ and IPS-$1^{-/-}$ mice even in this high-dose setting. However, IFN-α production was reproduced in a cell type level (peritoneal Mf) in vitro (Supplemental Fig. 1*C*). PV infection-mediated cell death (28) and degradation of MDA5 protein (29) may be major causes for this undetectable type I IFN production during in vivo PV infection.

TICAM-1 pathway contributes to IFN-β induction in WT mice with low PV titers

We next determined the mRNA levels of type I IFN in each organ extracted from PV (2×10^4 PFU)-infected WT and TICAM-$1^{-/-}$ mice. IFN-β mRNA was upregulated in all of the organs tested in WT mice within 12 h in response to PV injection (i.p.) (Fig. 4*A*). In contrast, only a low increase in IFN-β mRNA was detected in the organs of TICAM-$1^{-/-}$ mice (Fig. 4*A*). IFN-α2 mRNA was upregulated in the organs of TICAM-$1^{-/-}$ and WT mice to similar extents in response to PV injection (2×10^4 PFU, i.p.) (Fig. 4*B*). Notable decreases in IFN-α2 mRNA were observed in the TICAM-$1^{-/-}$ spleen and spinal cord compared with WT controls (Fig. 4*B*). The mRNA levels of genes associated with type I IFN induction were evaluated by qPCR, and no unique differences were observed between the splenocytes from PV-injected TICAM-$1^{-/-}$ and IPS-$1^{-/-}$ mice (Supplemental Fig. 1*D*). Hence, type I IFN mRNA is generally upregulated via TICAM-1 in the local organs of PVRtg WT mice during PV infection.

The mRNA levels of IFN-inducible genes and other cytokines were determined in spleen cells after PV infection. IFN-λ and IFN-γ–induced protein 10 (IP-10) mRNA were upregulated in the spleen cells of WT, but not TICAM-$1^{-/-}$ mice, after PV infection (multiplicity of infection [MOI] of 1) (Fig. 4*C*), with profiles similar to that of IFN-β mRNA (Fig. 4*C*). A sensor for 5′-triphosphorylated RNA, IFN-induced protein with tetratripeptide repeats 1 (IFIT-1), was also upregulated through PV infection (Fig. 4*C*). TNF-α, IL-10, IL-12p40, and IFN-γ, which may be associated with infectious cell death, were barely upregulated in spleen cells in response to PV infection (Supplemental Fig. 1*E*).

TICAM-1–dependent type I IFN induction by PV depends on Mf in PVRtg mice

The types of cells that participate in type I IFN induction in the spleen were examined by sorting spleen cells. IFN-β and IFN-α2 were found to be induced in WT $CD11c^+$ DC (Fig. 5*A*), whereas $CD11c^-$ cells barely induced type I IFN. Furthermore, IFN-β and IFN-α2 were barely induced in TICAM-$1^{-/-}$ $CD11c^+$ cells (Fig. 5*B*). Participation of IPS-1 in type I IFN induction in $CD11c^+$ myeloid cells is less compared with that of TICAM-1 (Fig. 5*B*).

Splenic $CD8\alpha^+CD11c^+$ and $CD4^+CD11c^+$ cells were separated by MACS beads and their response to PV (MOI of 1) was analyzed by determining the mRNA levels of type I IFN (Fig. 5*C*). $CD8\alpha^+CD11c^+$ cells, but not the $CD4^+CD11c^+$ cells, of WT mice were responsible for type I IFN induction by PV. There was a $CD4^-CD8\alpha^-$ population of DC in the spleen and this type of cells did not induce type I IFN in response to PV (Supplemental Fig. 2). The generation of the mRNA of type I IFN and IFIT-1 by PV infection was abrogated in the TICAM-$1^{-/-}$ $CD8\alpha^+CD11c^+$ splenic DC (Fig. 5*D*). Also, CD4/8α double-negative DC failed to express type I IFNs (Supplemental Fig. 2). Thus, $CD8\alpha^+CD11c^+$ DC, which reportedly express TLR3 (30), are the source of type I IFN in PV-infected PVRtg mice.

We finally confirmed that type I IFN is locally induced in $TLR3^+$ myeloid cells during PV infection. BM-Mf and BM-DC were prepared from mouse BM and challenged with PV (MOI of 1). These cells express TLR3 in the endosome as previously reported about mouse BM-DC (30) and human monocyte-derived DC (31). BM-Mf showed similar profiles of type I IFN mRNA to those of PV-infected splenocytes (Figs. 4*C*, 6*A*). However, IFN-λ and IP-10 mRNA were not detectable in PV-infected BM-Mf, the reason for which remains unclear (Fig. 6*A*). IL-12p40, a representative TICAM-1–dependent gene, was transiently upregulated

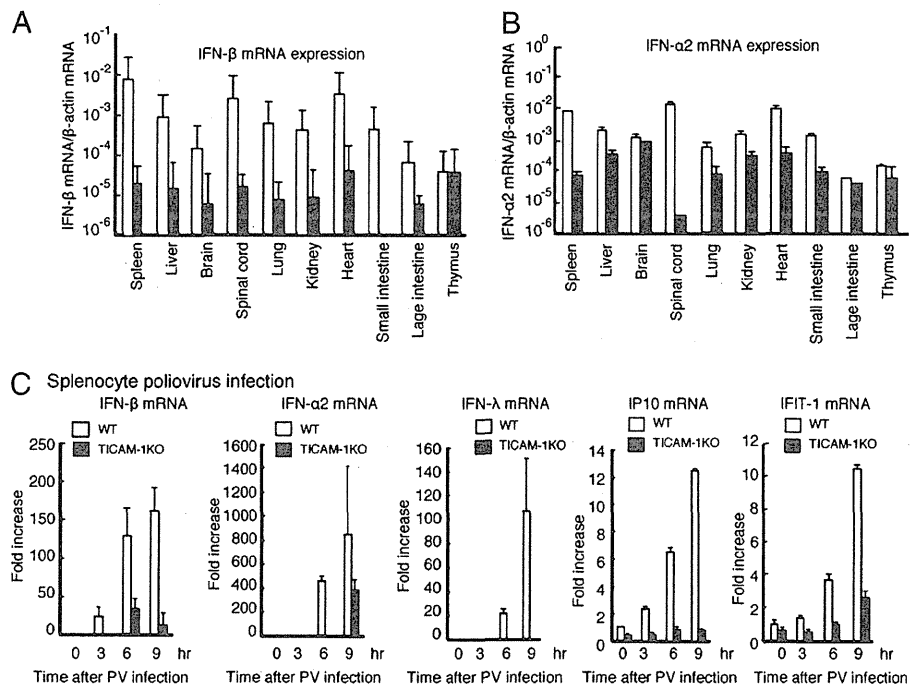

FIGURE 4. The expression of type I IFN following PV infection. *A* and *B*, WT and TICAM-1 KO mice were infected i.p. with 2×10^4 PFU PV. Three days postinfection, the mRNA expression levels of IFN-β (*A*) and IFN-α (*B*, *C*) were determined by RT-qPCR. *C*, Splenocytes (5×10^5) were infected with PV (MOI of 1) and the mRNA expression levels of IFN-β, IFN-α2, IFN-λ, IP-10, and IFIT-1 were measured by RT-qPCR. Data are shown as means ± SD and are representative of three independent experiments.

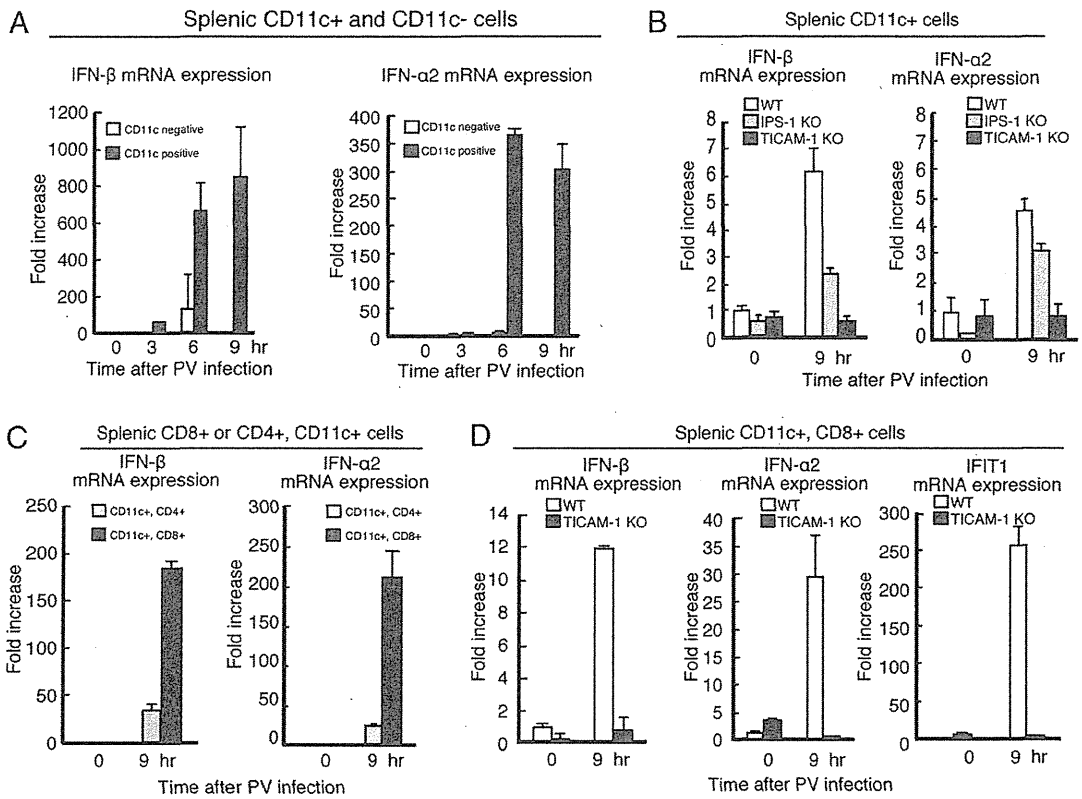

FIGURE 5. The expression of type I IFN in splenic DC. *A*, were isolated from WT spleens using the MACS system. $CD11c^+$ or $CD11c^-$ cells (5×10^5) were infected with PV (MOI of 1), and the mRNA expression of type I IFNs was measured by RT-qPCR. *B*, WT, TICAM-1, and IPS-1 knockout splenic $CD11c^+$ cells were infected with PV, and the expression of type I IFNs was measured by RT-qPCR. *C*, $CD8\alpha^+CD11c^+$ cells and $CD4^+CD11c^+$ cells were isolated from WT spleens and infected with PV (MOI of 1). The expression of type I IFNs was measured by RT-qPCR. *D*, $CD8\alpha^+CD11c^+$ splenic cells were isolated from WT and TICAM-1 KO mice and infected with PV (MOI of 1). The expressions of type I IFNs and IFIT-1 were measured by RT-qPCR. Data are shown as means ± SD and are representative of three independent experiments.

in BM-Mf ~4 h after PV infection (Supplemental Fig. 3). Similarly, but less prominently, the profiles of type I IFN and IL-12p40 were observed in BM-DC (Fig. 6*A*, Supplemental Fig. 3) and $CD11c^+CD8^+$ splenic DC (Fig. 5*D*). Therefore, taken together, these results indicate that IL-12 and IFN-α/β are only minimally upregulated in splenic DC in a PV-dependent manner.

The production of IFN-α was determined by ELISA in the supernatant of PV-infected BM-Mf and BM-DC (Fig. 6*C*). BM-Mf prepared from WT mice generated higher amounts of IFN-α than did those from TICAM-$1^{-/-}$ mice. Although similar results were obtained with BM-DC, the effect of TICAM-1 depletion was not statistically significant (Fig. 6*C*).

NK cells and MEF do not play major roles in protection against PV infection

Using NK1.1-depleted mice, we tested the possible participation of NK cells in the protection of PVRtg mice from PV infection (Fig. 7). $NK1.1^+$ cells were depleted from mouse blood 1 d after injection (i.p.) of NK1.1 Ab into WT (Fig. 7*A*) and TICAM-$1^{-/-}$ mice. After PV challenge, WT mice inoculated with control saline and NK1.1 Ab survived similarly, whereas TICAM-$1^{-/-}$ mice were all killed by PV within 7.5 d irrespective of NK1.1 pretreatment (Fig. 7*B*). Hence, NK cell activation does not affect PV-derived death. The lack of TICAM-1 was also found to have no effect on the NK cell-mediated rescue of PV-infected mice.

Mouse fibroblasts are known to be a potential source of type I IFN (13). We therefore checked whether MEF induce type I IFN and protection against PV (Supplemental Fig. 4). MEF from WT PVRtg mice were susceptible to PV, with cell death being observed at an MOI of 1. MEF from TICAM-$1^{-/-}$ PVRtg mice were 1 log more susceptible to PV, with cell death occurring at an MOI of 0.1 (Supplemental Fig. 4*A*). IFN-β was upregulated in PV-infected MEF to only a slightly higher level in PVRtg MEF than in TICAM-$1^{-/-}$ PVRtg MEF (Supplemental Fig. 4*B*). These results suggested that the large difference in the PV survival rate between WT and TICAM-$1^{-/-}$ mice is not caused by NK cells or type I IFN induction by fibroblasts. The TICAM-1 pathway plays a key role for producing IFN-α/β in Mf/DC, but not in fibroblasts, during PV infection in PVRtg mice.

Discussion

In this study, we demonstrated that PV infection is exacerbated in TICAM-$1^{-/-}$ PVRtg mice. There are a number of RNA-sensing molecules that serve as anti-virus agents and function in a cell type-specific manner. Based on trials using gene-disrupted mice and human viruses, RIG-I has been reported to be essential for sensing infection by rhabdoviruses, influenza viruses, paramyxoviruses, and flaviviruses, whereas MDA5 is important for sensing picornavirus infection (13, 33). In previous studies on picornaviruses, however, only EMCV and several species of picornaviruses have been employed for the KO mice analyses (13). The essential role of type I IFN in PV tropism has been well characterized in PVRtg mice (34). To our knowledge, this study is the first to investigate the sensor that detects PV infection in PVRtg PV-sensitive mice. Because RIG-I and MDA5 use the adaptor IPS-1, we constructed an IPS-$1^{-/-}$ mouse strain for this

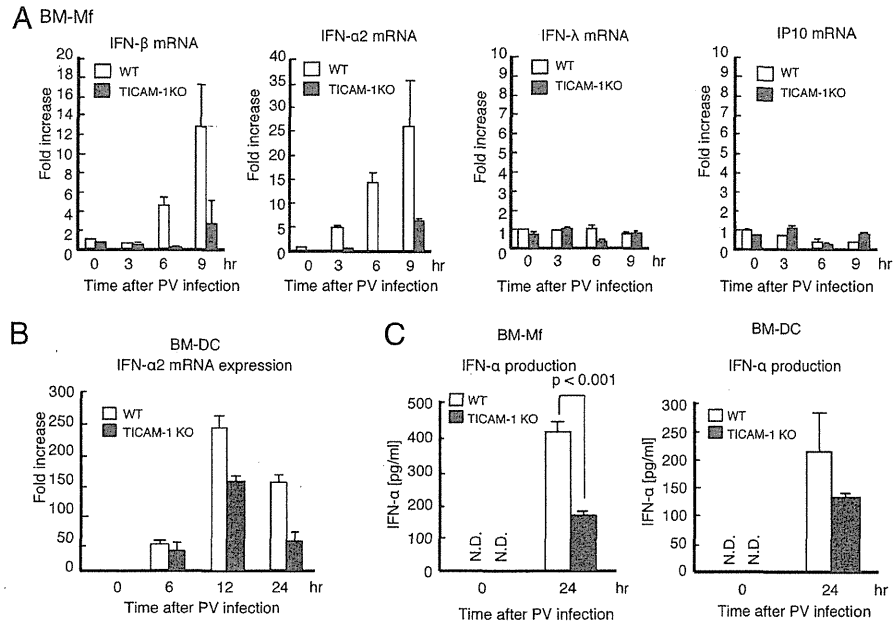

FIGURE 6. Production of type I IFN from BM-Mf and BM-DC. BM-Mf (*A*) and BM-DC (*B*) were prepared from BM cells with M-CSF and GM-CSF, respectively (32). The cells were infected with PV (MOI of 1), and the expression levels of IFN-β, IFN-α2, IFN-λ, and IP-10 were determined by RT-qPCR. *C*, IFN-α produced by PV-infected BM-Mf and BM-DC was measured by ELISA. BM-Mf and BM-DC were prepared from BM cells of WT and TICAM-1$^{-/-}$ mice as in *A* and *B*. Data are shown as means ± SD and are representative of three independent experiments.

study. Unexpectedly, however, IPS-1 was dispensable for protection against PV infection in vivo. This study, taken together with other reports (33, 35, 36), suggests that each virus species has its own strategy to evade host immune attack. This is true even in picornavirus subspecies. Although the IPS-1 pathway involving RIG-I and MDA5 is important for sensing and preventing cytoplasmic virus replication, other steps also participate in critical regulation of virus replication. PV infection is the case where MDA5 is not absolutely critical, but TICAM-1 is essential, for virus protection.

The TICAM-1 pathway participates in driving NK/CTL activation in DC/Mf (21, 37). This pathway is involved in type I IFN induction, as in the IPS-1 pathway, but cells expressing TLR3 are limited. The TLR3 distribution profile by flow cytometry confirms its expression in myeloid cells in mice (30). The TICAM-1 pathway converges with the IPS-1 pathway via the molecular complex of IRF-3–activating kinases (38), and therefore activation of the TICAM-1 pathway induces type I IFN and other IFN-inducible genes (39). Nevertheless, gene induction profiles differ between the TICAM-1 and IPS-1 pathways (40), which may explain the functional distinction between the sensor that is triggered in the virus-infected cells (MDA5/IPS-1) and the sensor that is required for DC/Mf to mount immune responses. Studying these gene functions will be an important issue for functional discrimination between the intrinsic versus extrinsic sensors.

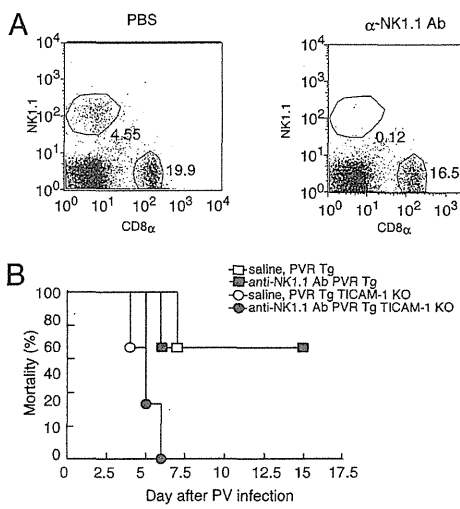

FIGURE 7. Effect of NK cells on mortality of PV-infected TICAM-1$^{-/-}$ PVRtg mice. *A*, To block the NK cell activity in mice, NK1.1 Ab or PBS (control) was i.p. injected into WT mice ($n \geq 6$). After 24 h, spleen cells were isolated from the mice and the fraction of NK1.1$^+$ cells was measured by FACS analysis. *B*, NK1.1 Ab or PBS was i.p. injected into WT and TICAM-1 KO mice. After 24 h, the mice were infected i.p. with PV, and survival was monitored for 15 d.

RIG-1/MDA5 are distributed over almost all organs, including Mf/DC. An interesting point concerns what the function is of the IPS-1 pathway in Mf/DC. Without conditional KO mice, we have an experimental limit to discriminate between their intrinsic function that is triggered in PV-infected cells and the extrinsic function leading Mf/DC to driving the innate immune response. Because the TLR3/TICAM-1 pathway is conserved in Mf/DC, the CNS, fibroblasts, and epithelical cells, it is reasonable that their functions are rather specified in Mf/DC and the neuronal system in PV infection.

However, except several examples such as rhabdovirus (41) and hepatitis C virus (HCV) (32), no definitive evidence has been reported supporting the role of TLR3/TICAM-1 in anti-RNA virus function using KO mice, unlike IPS-1 (35, 36). In previous studies, we used RNA viruses and their mouse models of measles virus, respiratory syncitial virus, vesicular stomatitis virus, influenza virus, and rotavirus infection (12), but we were unable to demonstrate solid antiviral function of the TLR3/TICAM-1 pathway in these models (12). Accordingly, which type I IFN, IFN-inducible gene, NK cell, or CTL is an effector for antagonizing viral replication still remains uncharacterized. To our knowledge, the results of our present study first demonstrated that the TLR3/TICAM-1 pathway is indispensable for induction of the type I IFN effector, but not NK cell activation, which is a critical event in the elimination of virus-infected cells and host protection against PV. IL-12 and IFN-γ are not upregulated in splenic DC in a PV-dependent manner. Furthermore, CTL are unlikely to be involved in our present model, since they would not function within the time scale of several days after initial infection (42).

How PV circumvents host-inducible type I IFN is an intriguing point. Three lines of evidence have supported the presence of unique mechanisms by which PV infection abrogates MDA5-mediated type I IFN production by infected cells and accelerates TLR3-mediated DC maturation through phagocytosis of PV-infected cell debris. First, proteases encoded in the PV genome process the PV polyprotein to produce functional viral proteins (43). PV 2A and 3C proteases also contribute to the degradation of eIF4G (44) and TATA-binding protein (45), respectively, the cleavage of which induces the translational and transcriptional "shutoff" of host protein synthesis (28). Thus, blocking the synthesis of host cell proteins by PV involves stopping IFN production. Second, MDA5 is degraded in PV-infected cells in a proteasome- and caspase-dependent manner, resulting in the lack of type I IFN production (29). Third, PV-mediated apoptosis occurs in a caspase-dependent manner to disable infected cells from inducing an IFN response (46), with the MDA5-dependent innate response to PV infection becoming minimal within 3 h postinfection. Additionally, RIG-I is also cleaved by the viral protease 3C (47), and additional RIG-I functions are subsequently disrupted. Hence, the RIG-I/MDA5 functional time frames should be narrow and ineffective in PV-infected cells.

The hijacked cells release virions and die irrespective of blocking of the IPS-1 pathway. These infected cells are degrading into apoptotic debris containing virus dsRNA when RIG-I/MDA5 is ineffective at inducing IFN (48). Phagocytic internalization of this infected debris containing viral dsRNA into endosomes in Mf/DC is a critical event for TLR3 stimulation (37). If this is the case in PV-infected PVRtg mice, dsRNA-containing debris produced by apoptosis of PV-infected cells may play a major role in the activation of the TICAM-1 pathway in myeloid cells, as is the case for another positive-stranded RNA virus, HCV (32). In HCV studies, dead cells act as carriers of viral dsRNA to the endosomes of DC (32). HCV induces cellular immunity including NK activation driven by the DC TICAM-1 pathway. PV, however, barely induces NK cell activation.

The results of the present study were obtained using the PVRtg mouse model for human PV infection. Possible limitations of this model may include the fact that PV natural infection in humans occurs postinfection of the intestine by a low dose of PV and the PV mouse model is unable to reproduce this infectious route (27). The difference in PV infection between human and the PVRtg mouse might reflect the difference of the IFN-inducing system in humans and mice. However, the response to neurovirulence and death by PV infection occurs similarly in mice and humans. PVRtg mice are susceptible to neuronal infection and the IFNAR$^{-/-}$ phenotype further enhances systemic PV infection (27, 34). The G (Sabin vaccine) and A forms (WT) of PV, which harbor G or A residues in their stem-loop V structures, respectively, show different levels of toxicity or neurovirulence (49). The lower toxicity of the vaccine strain is due to suppression of PTB-mediated protein synthesis in the G form. These results are essentially reproducible in the PVRtg mouse model (50). Our findings further indicate the essential role of the TICAM-1 pathway in the PVRtg model system for the PV-mediated induction of type I IFN in vivo. How this finding is associated with PV-mediated paralytic death and aberrance in the neuronal system is an open question for further understanding the PV neurovirulence and host defense.

In studies on virus infection in neurons, there was no difference between TLR3$^{-/-}$ and WT mice in the brain of reovirus infection (51). TLR3$^{-/-}$ mice have less severe neuroinvasiveness and survive longer than do WT mice in rabies virus infection (41). Further extensive studies have been performed with West Nile virus (WNV). TLR3$^{-/-}$ or TICAM-1$^{-/-}$ mice became more resistant to WNV infection than did WT mice (52). Compared to these earlier results, a recent report showed that lack of TLR3 enhances WNV mortality and increases viral burden in the brain (53). TNF-α and IL-6 are induced for inflammation, and high IL-10 production causes an increase of mortality in WNV-infected mice (54). TICAM-1 signaling is undoubtedly involved in the modulation of these cytokine productions and WNV replication in the nervous system (53, 54). In patients with herpes simplex encephalitis, functional deficiency of TLR3 or TICAM-1 is a critical factor for disease progression (55). The TLR3 responses in the CNS may differ from those in the immune system we examined (54, 56). How PV infection modulates IFN/cytokine-inducing signaling in the nervous system is an interesting issue. The possibility remains that cytokines, such as TNF-α, IL-10, IL-12p40, and IFN-γ, might be associated with the removal of infectious cells as in other virus infections, and the antiviral function of TLR3 ligands in PV-infected mice requires further elucidation.

A picornavirus CBV activates the TLR3/TICAM-1–IFN-γ axis in host-infected cells to induce type II IFN (18). It is possible that CBV promotes TLR3-dependent IFN-γ induction in lymphocytes rather than the type I IFN-inducing pathway. In the model of PV infection, however, the TICAM-1 pathway does not contribute to type II IFN induction. These findings indicate that picornaviruses, that is, EMCV, CBV and PV, have independently evolved to adapt to the host innate immune system and cope with the IFN-inducing system. If this is the case, host responses against picornaviruses may not be unimodally raised by MDA5 but may provide differentially adapted strategies. EMCV tropism reported previously (13) is clearly distinct from those of other picornaviruses. In this article, we present evidence that PV infection is protected by the TICAM-1 pathway that extrinsically induces type I IFN. Virus-produced dsRNA may differentially act on host cells depending on each virus species and accomplish circumvention from host innate sensing systems, maintaining virus tropism.

Acknowledgments

We are grateful to Dr. A. Nomoto (University of Tokyo, Tokyo, Japan) and our laboratory members for invaluable discussions. We also thank Dr. D.M. Segal (National Institutes of Health, Bethesda, MD) for providing us with anti-monse TLR3 mAb and Drs. S. Akira (Osaka University, Osaka, Japan) and T. Taniguchi (University of Tokyo) for providing TLR3$^{-/-}$ and IRF3/7$^{-/-}$ mice, respectively, for this study.

Disclosures

The authors have no financial conflicts of interest.

References

1. Takeuchi, O., and S. Akira. 2009. Innate immunity to virus infection. *Immunol. Rev.* 227: 75–86.
2. Malathi, K., B. Dong, M. Gale, Jr., and R. H. Silverman. 2007. Small self-RNA generated by RNase L amplifies antiviral innate immunity. *Nature* 448: 816–819.
3. Oshiumi, H., M. Matsumoto, K. Funami, T. Akazawa, and T. Seya. 2003. TICAM-1, an adaptor molecule that participates in Toll-like receptor 3-mediated interferon-β induction. *Nat. Immunol.* 4: 161–167.
4. Yamamoto, M., S. Sato, H. Hemmi, K. Hoshino, T. Kaisho, H. Sanjo, O. Takeuchi, M. Sugiyama, M. Okabe, K. Takeda, and S. Akira. 2003. Role of adaptor TRIF in the MyD88-independent Toll-like receptor signaling pathway. *Science* 301: 640–643.
5. Hoebe, K., X. Du, P. Georgel, E. Janssen, K. Tabeta, S. O. Kim, J. Goode, P. Lin, N. Mann, S. Mudd, et al. 2003. Identification of Lps2 as a key transducer of MyD88-independent TIR signalling. *Nature* 424: 743–748.
6. Akira, S. 2003. Toll-like receptor signaling. *J. Biol. Chem.* 278: 38105–38108.
7. Matsumoto, M., and T. Seya. 2008. TLR3: interferon induction by double-stranded RNA including poly(I:C). *Adv. Drug Deliv. Rev.* 60: 805–812.
8. Funami, K., M. Sasai, Y. Ohba, H. Oshiumi, T. Seya, and M. Matsumoto. 2007. Spatiotemporal mobilization of Toll/IL-1 receptor domain-containing adaptor molecule-1 in response to dsRNA. *J. Immunol.* 179: 6867–6872.
9. Funami, K., M. Sasai, H. Oshiumi, T. Seya, and M. Matsumoto. 2008. Homo-oligomerization is essential for Toll/interleukin-1 receptor domain-containing

adaptor molecule-1-mediated NF-κB and interferon regulatory factor-3 activation. *J. Biol. Chem.* 283: 18283–18291.
10. Yoneyama, M., M. Kikuchi, T. Natsukawa, N. Shinobu, T. Imaizumi, M. Miyagishi, K. Taira, S. Akira, and T. Fujita. 2004. The RNA helicase RIG-I has an essential function in double-stranded RNA-induced innate antiviral responses. *Nat. Immunol.* 5: 730–737.
11. Yoneyama, M., M. Kikuchi, K. Matsumoto, T. Imaizumi, M. Miyagishi, K. Taira, E. Foy, Y. M. Loo, M. Gale, Jr., S. Akira, et al. 2005. Shared and unique functions of the DExD/H-box helicases RIG-I, MDA5, and LGP2 in antiviral innate immunity. *J. Immunol.* 175: 2851–2858.
12. Matsumoto, M., H. Oshiumi, and T. Seya. 2011. Antiviral responses induced by the TLR3 pathway. *Rev. Med. Virol.* 21: 67–77.
13. Kato, H., O. Takeuchi, S. Sato, M. Yoneyama, M. Yamamoto, K. Matsui, S. Uematsu, A. Jung, T. Kawai, K. J. Ishii, et al. 2006. Differential roles of MDA5 and RIG-I helicases in the recognition of RNA viruses. *Nature* 441: 101–105.
14. Tabeta, K., P. Georgel, E. Janssen, X. Du, K. Hoebe, K. Crozat, S. Mudd, L. Shamel, S. Sovath, J. Goode, et al. 2004. Toll-like receptors 9 and 3 as essential components of innate immune defense against mouse cytomegalovirus infection. *Proc. Natl. Acad. Sci. USA* 101: 3516–3521.
15. Baltimore, D., Y. Becker, and J. E. Darnell. 1964. Virus-specific double-stranded RNA in poliovirus-infected cells. *Science* 143: 1034–1036.
16. Nomoto, A., B. Detjen, R. Pozzatti, and E. Wimmer. 1977. The location of the polio genome protein in viral RNAs and its implication for RNA synthesis. *Nature* 268: 208–213.
17. Gitlin, L., W. Barchet, S. Gilfillan, M. Cella, B. Beutler, R. A. Flavell, M. S. Diamond, and M. Colonna. 2006. Essential role of mda-5 in type I IFN responses to polyriboinosinic:polyribocytidylic acid and encephalomyocarditis picornavirus. *Proc. Natl. Acad. Sci. USA* 103: 8459–8464.
18. Negishi, H., T. Osawa, K. Ogami, X. Ouyang, S. Sakaguchi, R. Koshiba, H. Yanai, Y. Seko, H. Shitara, K. Bishop, et al. 2008. A critical link between Toll-like receptor 3 and type II interferon signaling pathways in antiviral innate immunity. *Proc. Natl. Acad. Sci. USA* 105: 20446–20451.
19. Ren, R. B., F. Costantini, E. J. Gorgacz, J. J. Lee, and V. R. Racaniello. 1990. Transgenic mice expressing a human poliovirus receptor: a new model for poliomyelitis. *Cell* 63: 353–362.
20. Koike, S., C. Taya, T. Kurata, S. Abe, I. Ise, H. Yonekawa, and A. Nomoto. 1991. Transgenic mice susceptible to poliovirus. *Proc. Natl. Acad. Sci. USA* 88: 951–955.
21. Akazawa, T., T. Ebihara, M. Okuno, Y. Okuda, M. Shingai, K. Tsujimura, T. Takahashi, M. Ikawa, M. Okabe, N. Inoue, et al. 2007. Antitumor NK activation induced by the Toll-like receptor 3-TICAM-1 (TRIF) pathway in myeloid dendritic cells. *Proc. Natl. Acad. Sci. USA* 104: 252–257.
22. Honda, K., H. Yanai, H. Negishi, M. Asagiri, M. Sato, T. Mizutani, N. Shimada, Y. Ohba, A. Takaoka, N. Yoshida, and T. Taniguchi. 2005. IRF-7 is the master regulator of type-I interferon-dependent immune responses. *Nature* 434: 772–777.
23. Kato, H., O. Takeuchi, E. Mikamo-Satoh, R. Hirai, T. Kawai, K. Matsushita, A. Hiiragi, T. S. Dermody, T. Fujita, and S. Akira. 2008. Length-dependent recognition of double-stranded ribonucleic acids by retinoic acid-inducible gene-I and melanoma differentiation-associated gene 5. *J. Exp. Med.* 205: 1601–1610.
24. Hornung, V., J. Ellegast, S. Kim, K. Brzózka, A. Jung, H. Kato, H. Poeck, S. Akira, K. K. Conzelmann, M. Schlee, et al. 2006. 5′-Triphosphate RNA is the ligand for RIG-I. *Science* 314: 994–997.
25. Pichlmair, A., O. Schulz, C. P. Tan, T. I. Näslund, P. Liljeström, F. Weber, and C. Reis e Sousa. 2006. RIG-I-mediated antiviral responses to single-stranded RNA bearing 5′-phosphates. *Science* 314: 997–1001.
26. Nakajima, A., K. Nishimura, Y. Nakaima, T. Oh, S. Noguchi, T. Taniguchi, and T. Tamura. 2009. Cell type-dependent proapoptotic role of Bcl2L12 revealed by a mutation concomitant with the disruption of the juxtaposed *Irf3* gene. *Proc. Natl. Acad. Sci. USA* 106: 12448–12452.
27. Ohka, S., H. Igarashi, N. Nagata, M. Sakai, S. Koike, T. Nochi, H. Kiyono, and A. Nomoto. 2007. Establishment of a poliovirus oral infection system in human poliovirus receptor-expressing transgenic mice that are deficient in α/β interferon receptor. *J. Virol.* 81: 7902–7912.
28. Racaniello, V. R. 2007. Picornaviridae: the viruses and their replication. In *Fields Virology*, 5th Ed. D. M. Knipe and P. M. Howley, eds. Lippincott Williams & Wilkins, Philadelphia, p. 795–838.
29. Barral, P. M., J. M. Morrison, J. Drahos, P. Gupta, D. Sarkar, P. B. Fisher, and V. R. Racaniello. 2007. MDA-5 is cleaved in poliovirus-infected cells. *J. Virol.* 81: 3677–3684.
30. Jelinek, I., J. N. Leonard, G. E. Price, K. N. Brown, A. Meyer-Manlapat, P. K. Goldsmith, Y. Wang, D. Venzon, S. L. Epstein, and D. M. Segal. 2011. TLR3-specific double-stranded RNA oligonucleotide adjuvants induce dendritic cell cross-presentation, CTL responses, and antiviral protection. *J. Immunol.* 186: 2422–2429.
31. Matsumoto, M., K. Funami, M. Tanabe, H. Oshiumi, M. Shingai, Y. Seto, A. Yamamoto, and T. Seya. 2003. Subcellular localization of Toll-like receptor 3 in human dendritic cells. *J. Immunol.* 171: 3154–3162.
32. Ebihara, T., M. Shingai, M. Matsumoto, T. Wakita, and T. Seya. 2008. Hepatitis C virus-infected hepatocytes extrinsically modulate dendritic cell maturation to activate T cells and natural killer cells. *Hepatology* 48: 48–58.
33. Loo, Y. M., J. Fornek, N. Crochet, G. Bajwa, O. Perwitasari, L. Martinez-Sobrido, S. Akira, M. A. Gill, A. García-Sastre, M. G. Katze, and M. Gale, Jr. 2008. Distinct RIG-I and MDA5 signaling by RNA viruses in innate immunity. *J. Virol.* 82: 335–345.
34. Ida-Hosonuma, M., T. Iwasaki, T. Yoshikawa, N. Nagata, Y. Sato, T. Sata, M. Yoneyama, T. Fujita, C. Taya, H. Yonekawa, and S. Koike. 2005. The α/β interferon response controls tissue tropism and pathogenicity of poliovirus. *J. Virol.* 79: 4460–4469.
35. Kumar, H., T. Kawai, H. Kato, S. Sato, K. Takahashi, C. Coban, M. Yamamoto, S. Uematsu, K. J. Ishii, O. Takeuchi, and S. Akira. 2006. Essential role of IPS-1 in innate immune responses against RNA viruses. *J. Exp. Med.* 203: 1795–1803.
36. Sun, Q., L. Sun, H. H. Liu, X. Chen, R. B. Seth, J. Forman, and Z. J. Chen. 2006. The specific and essential role of MAVS in antiviral innate immune responses. *Immunity* 24: 633–642.
37. Schulz, O., S. S. Diebold, M. Chen, T. I. Näslund, M. A. Nolte, L. Alexopoulou, Y. T. Azuma, R. A. Flavell, P. Liljeström, and C. Reis e Sousa. 2005. Toll-like receptor 3 promotes cross-priming to virus-infected cells. *Nature* 433: 887–892.
38. Sasai, M., M. Shingai, K. Funami, M. Yoneyama, T. Fujita, M. Matsumoto, and T. Seya. 2006. NAK-associated protein 1 participates in both the TLR3 and the cytoplasmic pathways in type I IFN induction. *J. Immunol.* 177: 8676–8683.
39. Oshiumi, H., M. Sasai, K. Shida, T. Fujita, M. Matsumoto, and T. Seya. 2003. TIR-containing adapter molecule (TICAM)-2, a bridging adapter recruiting to Toll-like receptor 4 TICAM-1 that induces interferon-beta. *J. Biol. Chem.* 278: 49751–49762.
40. Ueta, M., T. Kawai, N. Yokoi, S. Akira, and S. Kinoshita. 2011. Contribution of IPS-1 to polyI:C-induced cytokine production in conjunctival epithelial cells. *Biochem. Biophys. Res. Commun.* 404: 419–423.
41. Ménager, P., P. Roux, F. Mégret, J. P. Bourgeois, A. M. Le Sourd, A. Danckaert, M. Lafage, C. Préhaud, and M. Lafon. 2009. Toll-like receptor 3 (TLR3) plays a major role in the formation of rabies virus Negri bodies. *PLoS Pathog.* 5: e1000315.
42. Sigal, L. J., S. Crotty, R. Andino, and K. L. Rock. 1999. Cytotoxic T-cell immunity to virus-infected non-haematopoietic cells requires presentation of exogenous antigen. *Nature* 398: 77–80.
43. Nicklin, M. J., H. G. Kräusslich, H. Toyoda, J. J. Dunn, and E. Wimmer. 1987. Poliovirus polypeptide precursors: expression in vitro and processing by exogenous 3C and 2A proteinases. *Proc. Natl. Acad. Sci. USA* 84: 4002–4006.
44. Kräusslich, H. G., M. J. Nicklin, H. Toyoda, D. Etchison, and E. Wimmer. 1987. Poliovirus proteinase 2A induces cleavage of eucaryotic initiation factor 4F polypeptide p220. *J. Virol.* 61: 2711–2718.
45. Clark, M. E., P. M. Lieberman, A. J. Berk, and A. Dasgupta. 1993. Direct cleavage of human TATA-binding protein by poliovirus protease 3C in vivo and in vitro. *Mol. Cell. Biol.* 13: 1232–1237.
46. Belov, G. A., L. I. Romanova, E. A. Tolskaya, M. S. Kolesnikova, Y. A. Lazebnik, and V. I. Agol. 2003. The major apoptotic pathway activated and suppressed by poliovirus. *J. Virol.* 77: 45–56.
47. Barral, P. M., D. Sarkar, P. B. Fisher, and V. R. Racaniello. 2009. RIG-I is cleaved during picornavirus infection. *Virology* 391: 171–176.
48. Barco, A., E. Feduchi, and L. Carrasco. 2000. Poliovirus protease $3C^{pro}$ kills cells by apoptosis. *Virology* 266: 352–360.
49. Kawamura, N., M. Kohara, S. Abe, T. Komatsu, K. Tago, M. Arita, and A. Nomoto. 1989. Determinants in the 5′ noncoding region of poliovirus Sabin 1 RNA that influence the attenuation phenotype. *J. Virol.* 63: 1302–1309.
50. Koike, S., H. Horie, Y. Sato, I. Ise, C. Taya, T. Nomura, I. Yoshioka, H. Yonekawa, and A. Nomoto. 1993. Poliovirus-sensitive transgenic mice as a new animal model. *Dev. Biol. Stand.* 78: 101–107.
51. Edelmann, K. H., S. Richardson-Burns, L. Alexopoulou, K. L. Tyler, R. A. Flavell, and M. B. A. Oldstone. 2004. Does Toll-like receptor 3 play a biological role in virus infections? *Virology* 322: 231–238.
52. Wang, T., T. Town, L. Alexopoulou, J. F. Anderson, E. Fikrig, and R. A. Flavell. 2004. Toll-like receptor 3 mediates West Nile virus entry into the brain causing lethal encephalitis. *Nat. Med.* 10: 1366–1373.
53. Daffis, S., M. A. Samuel, M. S. Suthar, M. Gale, Jr., and M. S. Diamond. 2008. Toll-like receptor 3 has a protective role against West Nile virus infection. *J. Virol.* 82: 10349–10358.
54. Bai, F., T. Town, F. Qian, P. Wang, M. Kamanaka, T. M. Connolly, D. Gate, R. R. Montgomery, R. A. Flavell, and E. Fikrig. 2009. IL-10 signaling blockade controls murine West Nile virus infection. *PLoS Pathog.* 5: e1000610.
55. Zhang, S. Y., E. Jouanguy, S. Ugolini, A. Smahi, G. Elain, P. Romero, D. Segal, V. Sancho-Shimizu, L. Lorenzo, A. Puel, et al. 2007. TLR3 deficiency in patients with herpes simplex encephalitis. *Science* 317: 1522–1527.
56. Préhaud, C., F. Mégret, M. Lafage, and M. Lafon. 2005. Virus infection switches TLR-3-positive human neurons to become strong producers of beta interferon. *J. Virol.* 79: 12893–12904.

Figure S1

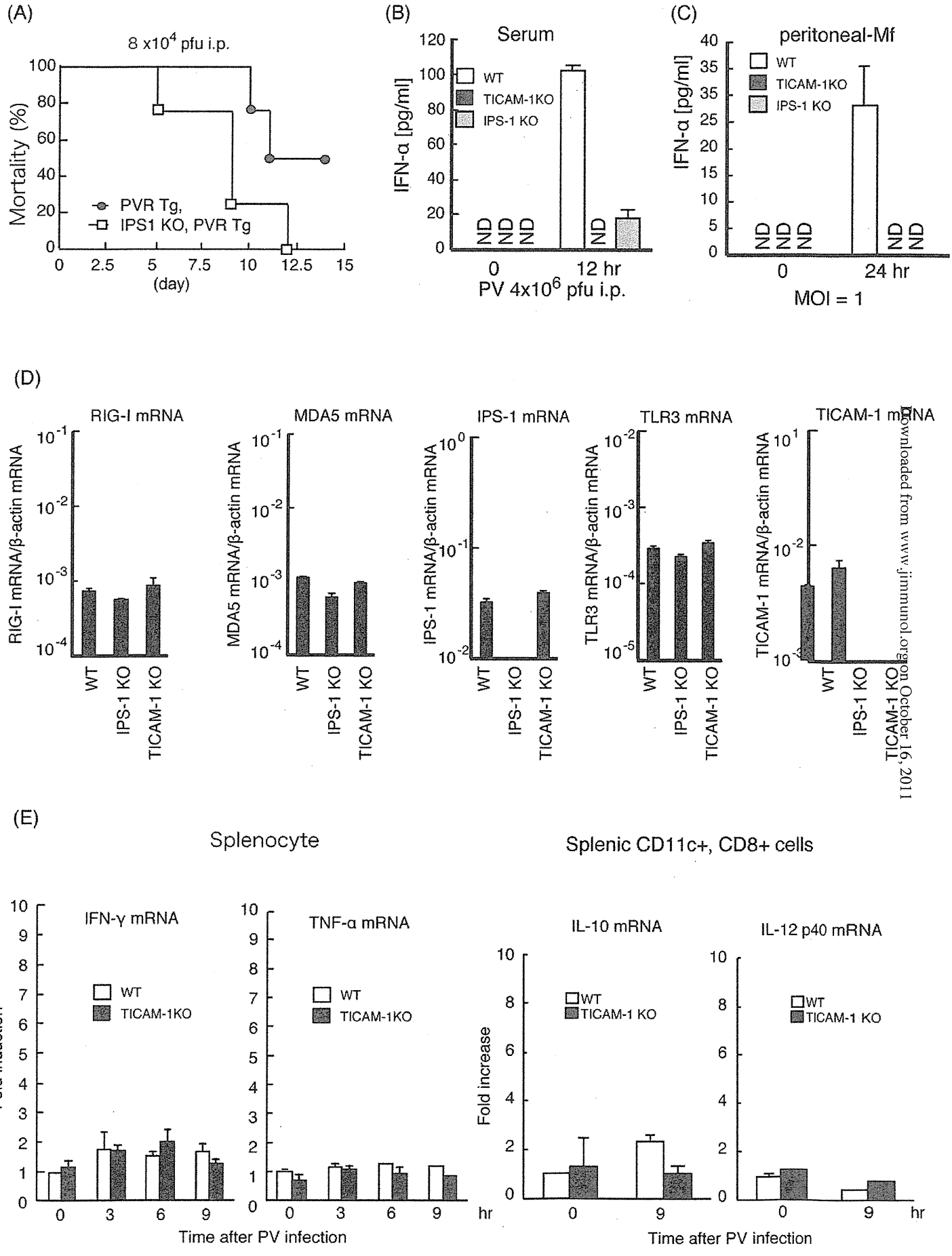

Figure S2

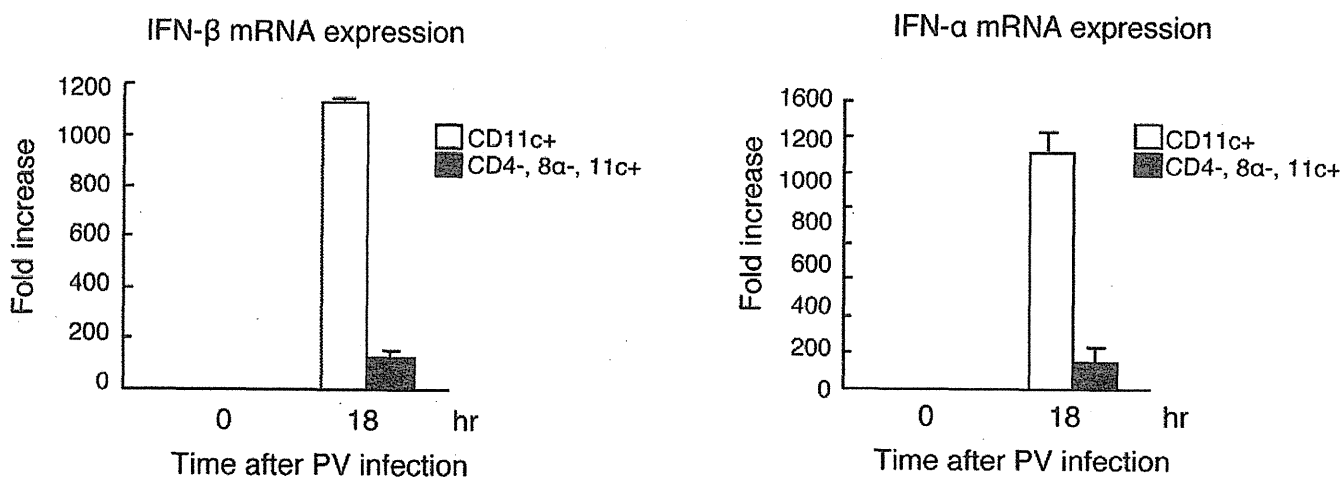

Figure S3

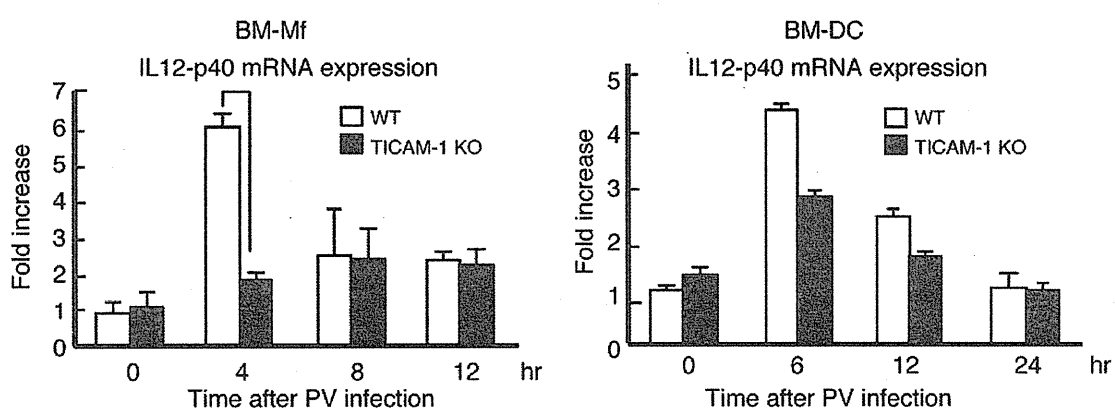

Figure S4

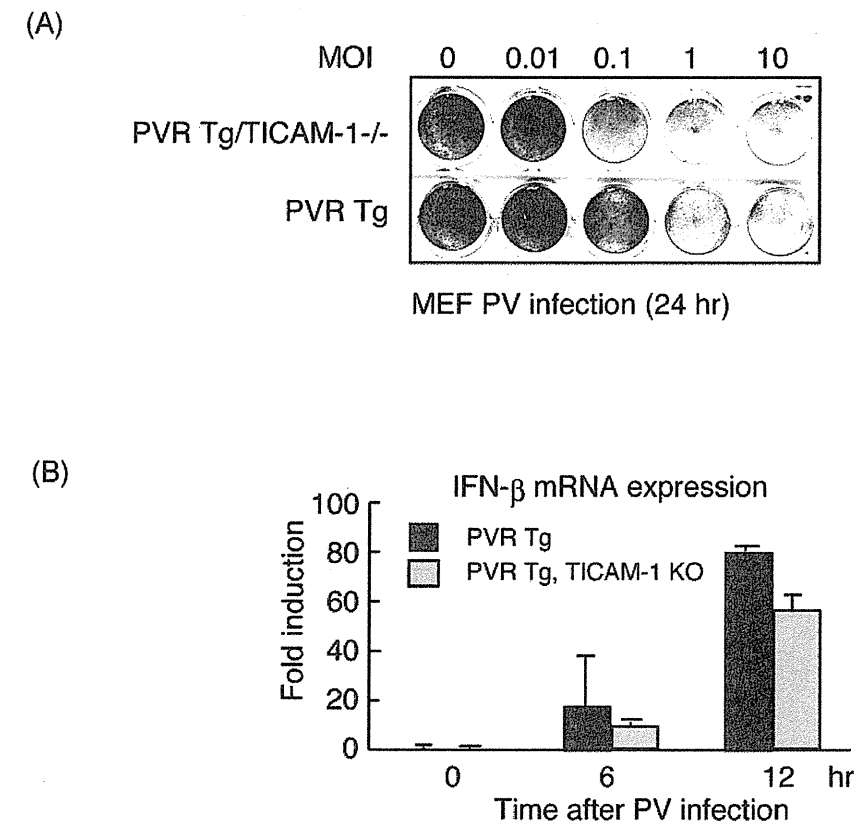

Supplemental figure legends

Figure S1. Production of IFN-α following PV infection. (A) 8×10^4 pfu of PV were intraperitoneally injected into wild-type and IPS-1 knockout (KO) mice, and the survival was monitored for 14 days. n=4. (B) 4×10^6 pfu of PV was intravenously injected into wild-type (WT), TICAM-1 knockout (KO) mice, and IPS-1 knockout mice (KO), and the cytokine levels in sera were measured by ELISA. (C) Peritoneal macrophages (peritoneal-Mf) (41) were induced from WT, TICAM-1 KO, and IPS-1 KO mice, and infected with PV (MOI=1) in a 24-well plate. The concentrations of IFN-α in the culture supernatants were measured by ELISA. (D) Splenocytes were isolated from WT, IPS-KO and TICAM-1 KO mice, and the expression of RIG-I, MDA5, TLR3, TICAM-1 and IPS-1 was measured by RT–qPCR. Data are shown as means ± SD and are representative of three independent experiments. (E) Splenocytes and CD8α+/CD11c+ cells were isolated from WT and TICAM-1 KO mice, and the expression levels of IFN-γ, IP-10, TNF-α, and IL-12 p40 were measured by RT–qPCR. Data are shown as means ± SD and are representative of three independent experiments.

Figure S2. No induction of type I IFN by CD4–/CD8α–/CD11C+ splenic dendritic cells (DC) was observed in response to PV. Splenocytes were harvested from PVRtg wild-type (WT) mice 18 h post PV intraperitoneal infection. Total CD11c+ cells and CD4–/CD8α–/CD11C+ cells were separated by flow cytometry. Fold increases in IFN mRNA were determined by RT–qPCR. Data are shown as means ± SD and are representative of three independent experiments.

Figure S3. IL-12p40 induced by PV infection in Mf. Bone marrow (BM)-macrophages (Mf) and BM-dendritic cells (DC) were prepared from the BM cells of wild-type and TICAM-1 knockout mice, and were infected with PV (MOI=1) in a 24-well plate. The expression of IL-12 p40 was measured by RT–qPCR. Data are shown as means ± SD and are representative of three independent experiments.

Figure S4. TICAM-1 was not a strong inducer for IFN-β in mouse embryonic fibroblasts (MEF). (A) Wild-type (WT) and TICAM-1 knockout (KO) MEF were infected with PV at the indicated MOI for 24 h. The cells were fixed and stained with

crystal violet. WT and TICAM-1 KO MEF were infected with PV (MOI=1), and the expression of IFN-β was measured by RT–qPCR. Data are shown as means ± SD and are representative of three independent experiments.

MOLECULAR AND CELLULAR BIOLOGY, Sept. 2011, p. 3802–3819 Vol. 31, No. 18
0270-7306/11/$12.00 doi:10.1128/MCB.01368-10

DDX60, a DEXD/H Box Helicase, Is a Novel Antiviral Factor Promoting RIG-I-Like Receptor-Mediated Signaling▽†

Moeko Miyashita,[1,2] Hiroyuki Oshiumi,[1]* Misako Matsumoto,[1] and Tsukasa Seya[1]

Department of Microbiology and Immunology, Graduate School of Medicine,[1] and Graduate School of Life Science,[2] Hokkaido University, Kita-15, Nishi-7, Kita-ku, Sapporo 060-8638, Japan

Received 30 November 2010/Returned for modification 27 December 2010/Accepted 12 July 2011

The cytoplasmic viral RNA sensors RIG-I and MDA5 are important for the production of type I interferon and other inflammatory cytokines. DDX60 is an uncharacterized DEXD/H box RNA helicase similar to *Saccharomyces cerevisiae* Ski2, a cofactor of RNA exosome, which is a protein complex required for the integrity of cytoplasmic RNA. Expression of DDX60 increases after viral infection, and the protein localizes at the cytoplasmic region. After viral infection, the DDX60 protein binds to endogenous RIG-I protein. The protein also binds to MDA5 and LGP2 but not to the downstream factors IPS-1 and IκB kinase ε (IKK-ε). Knockdown analysis shows that DDX60 is required for RIG-I- or MDA5-dependent type I interferon and interferon-inducible gene expression in response to viral infection. However, DDX60 is dispensable for TLR3-mediated signaling. Purified DDX60 helicase domains possess the activity to bind to viral RNA and DNA. Expression of DDX60 promotes the binding of RIG-I to double-stranded RNA. Taken together, our analyses indicate that DDX60 is a novel antiviral helicase promoting RIG-I-like receptor-mediated signaling.

RIG-I and MDA5 are cytoplasmic viral RNA sensors belonging to the group of RIG-I-like receptors (RLRs), which includes LGP2 (57–59). RIG-I recognizes RNAs from vesicular stomatitis virus (VSV), hepatitis C virus (HCV), Sendai virus (SeV), and influenza A virus (21, 36, 37), while MDA5 recognizes RNA from picornaviruses such as encephalomyocarditis virus and poliovirus (PV) (3, 19, 21). RLRs are also involved in the recognition of cytoplasmic B-DNA. RNA polymerase III transcribes cytoplasmic AT-rich double-stranded DNA (dsDNA), and the transcribed RNA is recognized by RIG-I (1, 6). In contrast, Choi et al. have reported that RIG-I associates with dsDNA (7).

When RIG-I or MDA5 is activated by viral infection, the N-terminal caspase recruitment domains (CARDs) associate with the adaptor protein IPS-1 (also called MAVS/Cardif/VISA) on the outer mitochondrial membrane (22, 26, 42, 55). After this association occurs, IPS-1 activates TBK1 and IκB kinase ε (IKK-ε) and signals interferon (IFN) regulatory factor 3 (IRF-3)- and NF-κB-responsive genes, such as those for type I IFNs or other inflammatory cytokines (22, 23, 26, 42, 44, 55).

Both the helicase and C-terminal domain (CTD) of RIG-I bind to RNA, but it is the CTD that is responsible for the recognition of the 5′ triphosphate double-stranded structure typical of viral RNA (16, 39, 40). Recently, Rehwinkel et al. showed that the physiological ligand of RIG-I during influenza A virus or SeV infection is the full-length viral genomic single-stranded RNA (ssRNA), which possesses base-paired regions or defective interfering (DI) genomes (35). In contrast to RIG-I, MDA5 recognizes long viral double-stranded RNA (dsRNA) (21). The RNA binding activity of the MDA5 CTD is relatively weak compared with that of the RIG-I CTD, because the basic surface of the MDA5 CTD has a more extensive flat region than the RIG-I CTD (8, 45, 46). Although the RNA binding activity of the MDA5 CTD is weak, this protein plays a pivotal role in the recognition of picornavirus RNA (20, 21).

For the efficient recognition of viral RNA, RIG-I and MDA5 require protein modification and association with upstream factors. LGP2 is one of the upstream factors. LGP2 lacks an N-terminal CARD; thus, LGP2 itself cannot transmit the signal in the absence of RIG-I or MDA5 (36, 38, 49). The CTD of LGP2, which binds to the terminal region of viral double-stranded RNA, is more similar to the CTD of RIG-I than to that of MDA5 (24, 33, 45). LGP2 knockout studies have revealed that LGP2 is essential for type I IFN production by MDA5 but plays only a minor role in type I IFN production by RIG-I (38, 49). RIG-I requires modification of K63-linked polyubiquitination by TRIM25 and Riplet/REUL ubiquitin ligases for its full activation (11, 13, 30, 31). High-mobility-group box (HMGB) proteins also act as upstream factors of RLRs. Recently, Yanai and colleagues reported that HMGB1, HMGB2, and HMGB3 serve as sentinels for the nucleic acids required for both RIG-I and MDA5 recognition of viral RNA (56). Hayakawa and colleagues reported that ZAPS associates with RIG-I to promote oligomerization and ATPase activity of RIG-I (15). Another factor interacting with RLRs is DDX3, a DEXD/H box RNA helicase, which is similar to LGP2 in that it does not contain a CARD but promotes signaling by forming a complex with either RIG-I or MDA5 (32). DDX3 also plays important roles in TBK-1- and IKK-ε-mediated IRF activation, and Schröder et al. and Soulat et al. were the first to describe results showing that DDX3 is a non-RLR helicase involved in innate immune responses (41, 43).

DDX60, a DEXD/H box helicase, was annotated in a genome project, and the protein function is unknown. The protein is weakly similar to SKIV2L and SKIV2L2 and is the

* Corresponding author. Mailing address: Department of Microbiology and Immunology, Graduate School of Medicine, Hokkaido University, Kita-15, Nishi-7, Kita-ku, Sapporo 060-8638, Japan. Phone: 81-11-706-5056. Fax: 81-11-706-7866. E-mail: oshiumi@med.hokudai.ac.jp.

† Supplemental material for this article may be found at http://mcb.asm.org/.

▽ Published ahead of print on 2 May 2011.